CrossMark

An in vitro alveolar macrophage assay for predicting the short-term inhalation toxicity of nanomaterials

Martin Wiemann[1*], Antje Vennemann[1], Ursula G. Sauer[2], Karin Wiench[3], Lan Ma-Hock[3] and Robert Landsiedel[3]

Abstract

Background: Most in vitro studies investigating nanomaterial pulmonary toxicity poorly correlate to in vivo inhalation studies. Alveolar macrophages (AMs) play an outstanding role during inhalation exposure since they effectively clear the alveoli from particles. This study addresses the applicability of an in vitro alveolar macrophage assay to distinguish biologically active from passive nanomaterials.

Methods: Rat NR8383 alveolar macrophages were exposed to 18 inorganic nanomaterials, covering AlOOH, $BaSO_4$, CeO_2, Fe_2O_3, TiO_2, ZrO_2, and ZnO NMs, amorphous SiO_2 and graphite nanoplatelets, and two nanosized organic pigments. ZrO_2 and amorphous SiO_2 were tested without and with surface functionalization. Non-nanosized quartz DQ12 and corundum were used as positive and negative controls, respectively. The test materials were incubated with the cells in protein-free culture medium. Lactate dehydrogenase, glucuronidase, and tumour necrosis factor alpha were assessed after 16 h. In parallel, H_2O_2 was assessed after 1.5 h. Using the no-observed-adverse-effect concentrations (NOAECs) from available rat short-term inhalation studies (STIS), the test materials were categorized as active (NOAEC < 10 mg/m^3) or passive.

Results: In vitro data reflected the STIS categorization if a particle surface area-based threshold of <6000 mm^2/mL was used to determine the biological relevance of the lowest observed significant in vitro effects. Significant effects that were recorded above this threshold were assessed as resulting from test material-unspecific cellular 'overload'. Test materials were assessed as active if ≥ 2 of the 4 in vitro parameters undercut this threshold. They were assessed as passive if 0 or 1 parameter was altered. An overall assay accuracy of 95 % was achieved.

Conclusions: The in vitro NR8383 alveolar macrophage assay allows distinguishing active from passive nanomaterials. Thereby, it allows determining whether in vivo short-term inhalation testing is necessary for hazard assessment. Results may also be used to group nanomaterials by biological activity. Further work should aim at validating the assay.

Keywords: Alveolar macrophages, NR8383 cells, Nanotoxicology, In vitro–in vivo comparison, Inhalation toxicity, 3Rs principle

Background

With the advent of nanotechnology, the importance of adequately assessing the human health impacts of nanomaterials (NMs) is widely recognized. Generally, NMs are covered by chemicals legislation, such as the EU regulation no. 1907/2006 on the registration, evaluation, authorisation and restriction of chemicals (REACH [1]). Taking into account the abundance of NM modifications in regard to particle size, shape, or surface properties and the very broad definition for 'nanomaterial' as it has been laid down, e.g., in EU Commission [2], it is expected that the safety of a substantial number of NMs will have to be assessed to meet the REACH information requirements [3]. At the same time, however, the REACH regulation

*Correspondence: martin.wiemann@ibe-ms.de
[1] IBR R&D gGmbH Institute for Lung Health, Mendelstraße 11, 48149 Münster, Germany
Full list of author information is available at the end of the article

Wiemann *et al. J Nanobiotechnol (2016) 14:16*

Page 2 of 27

requires that animal testing should only be undertaken as a last resort. Concordantly, Directive 2010/63/EU on the protection of animals used for scientific purposes [4] prescribes implementation of the 3Rs principle to replace, reduce and refine animal testing [5].

To promote the collection of relevant data for the safety assessment of a representative set of NMs, the Organisation for Economic Co-operation and Development Working Party on Manufactured Nanomaterials (OECD WPMN) has launched a Sponsorship Programme for the testing of manufactured nanomaterials [6, 7]. This programme further aims at establishing the role of 3Rs methods for NM testing [6]. With inhalation generally being one of the main routes of NM exposure both for workers and consumers [8, 9], the WPMN has proposed a short-term rat inhalation study (STIS [10]) as a suitable test method to reduce and refine repeated-dose sub-acute inhalation toxicity testing. The STIS provides information on early elements of NM-induced pathogenesis as well as on the reversibility, persistence or progression of effects. Furthermore, NM lung burden and potential for extra-pulmonary translocation may be investigated in the STIS [9–11].

Although the STIS allows reducing animal numbers, suffering, and distress as compared to the 28-day sub-acute inhalation toxicity study described in OECD Test Guideline (TG) 412 [12], it still uses sentient animals. There is also no in vitro test method available that may be used in a tiered approach to decide whether or not in vivo testing, beginning with the STIS, should be required for regulatory hazard assessment. Up to now, numerous different in vitro test systems encompassing submersed or air–liquid exposed cells of mostly pulmonary origin have been investigated in combination with a variety of different endpoint detection methods [13–20]. However, the available in vitro results are inconsistent, and to the best of the authors' knowledge, there is no in vitro assay that allows reliably predicting the in vivo effects of inhaled NMs [21].

Against this background, it was the goal of the current study to develop an in vitro assay that is suitable for routine regulatory testing of NM inhalation toxicity. In choosing an appropriate test system, it was taken into account which pulmonary cells are predominantly exposed to inhaled NMs. Depending on their aerodynamic diameter, inhaled particles may reach the deep regions of the pulmonary parenchyma [22]. Upon interaction with lung surfactant proteins and lipids, dispersed or agglomerated particles may deposit on the inner alveolar surface. In contrast to the bronchial walls that are protected by a mucus layer which is expelled by the underlying ciliated epithelium, alveolar cells are much more vulnerable. Nevertheless, within the alveoli particles may be engulfed by alveolar macrophages (AMs), which may then be removed via the mucociliary escalator [23–26]. Although nanoparticles were originally believed to be too small to be rapidly cleared by AMs, the dominant role of these cells for the uptake and clearance also of nanoparticles has been shown in various studies [27–29] and is now widely accepted. Only a very small fraction of inhaled NMs appears to permeate the intact lung epithelial barrier thereby potentially becoming systemically available [30–33]. It has also been suggested that nanoparticles may transiently enter the alveolar epithelium or the interstitium, thereby delaying sequestration by AMs [34–36]. Although the full details of the early steps of NM deposition, lung surfactant interaction, and particle transport are still under investigation, it goes undisputed that AMs harbour the major fraction of inhaled NMs, at least after acute or sub-acute exposure [35, 37], and that these cells play a central role in clearing the lung from inhaled NMs.

A multitude of endpoints may be studied to evaluate the biological responses of AMs that are exposed to NMs. AMs are specialized to fend off microbial invasions by non-specific, nicotinamide adenine dinucleotide phosphate-oxidase (NAPDH) oxidase-regulated oxidative burst. Unsurprisingly, also inhaled particles may elicit this type of response, at least upon increased particle load [38, 39]. Formation of extracellular reactive oxygen species (ROS) may elicit indirect oxidative damage of adjacent cells [40]. Moreover, AMs, forming part of the non-specific immune system, may initiate and orchestrate immunological processes by releasing chemokines and cytokines [41]. Together with the formation of extracellular ROS/H_2O_2 and/or nitrogen monoxide, AMs are known to release different pro-inflammatory mediators (e.g., tumour necrosis factor α (TNF-α); interleukins (IL-1, IL-6, IL-8); or monocyte chemoattractant protein-1 (MCP-1)) and fibrogenic mediators [e.g., transforming growth factor β (TGF-b); osteopontin; or platelet-derived growth factor (PDGF)] [10, 11, 41–45]. Some of these mediators may serve as chemoattractants for blood granulocytes, or they may enhance pulmonary inflammatory processes [46]. Likewise, AMs may release lytic and other enzymes upon (nano)particle stimulation which in return may activate or stimulate exocytosis [47–49].

Bioactive particles or high particle load may also impair macrophage functions, such as their motility or bactericidal capacity, which may eventually lead to the disruption of cell membrane integrity [23, 24, 50–52]. Although AMs are readily recruited from blood monocytes, any weakening of the intra-pulmonary AM population will affect lung clearance thereby enhancing the risk for the evolvement of lung diseases [53].

Wiemann *et al. J Nanobiotechnol (2016) 14:16*

Page 3 of 27

Since the pulmonary effects of NMs upon short-term inhalation exposure are predominantly AM-mediated, it appears promising to study essential biological responses of AMs in vitro when aiming at predicting in vivo short-term inhalation effects. This principle was established long before the term nanotoxicology was coined. Rehn et al. [54, 55] incubated a defined number of primary AMs lavaged from the lungs of guinea pigs and rats with a defined mass of micron-scaled particulate matter, such that a mean particle burden/AM could be calculated. Rehn et al. [55] designed their in vitro studies to cover the plausible in vivo particle burden/AM inside the rat lung. Assuming that the upper in vitro threshold corresponds to the upper in vivo rat lung threshold since primary rat AMs widely resemble in vivo rat AMs and these cells sequester the vast majority of inhaled particles, the relevant concentration range was estimated from the maximum rat lung burden divided by the number of AMs/lung. This number is fairly constant (i.e., $1-2 \times 10^7$) in healthy, unrestrained rats [55, 56]. Accordingly, Bruch et al. [57] calculated a mean particle burden of ≤ 120 pg/AM as a realistic in vivo upper value. Interestingly, direct measurements carried out on AMs extracted from the bronchoalveolar lavage fluid (BALF) of rats exposed to 30 mg/m^3 poorly soluble AlOOH NMs by inhalation for 28 days revealed a cell burden of approx. 90 pg/AM [58]. Altogether, these findings underline that cultured AMs may be exposed to doses that resemble in vivo conditions. This is a promising starting point for in vitro-in vivo comparisons.

An in vitro assay suitable for regulatory toxicity testing should include biologically relevant, but easy to measure endpoints. This will increase the predictive value of the in vitro data. The model originally proposed by Rehn et al. [55] comprised TNF-α (as a major pro-inflammatory cytokine), ROS/H$_2$O$_2$ (as a major inducer of oxidative stress), β-glucuronidase (GLU; indicating macrophage activation [44] and/or membrane damage), and AM bactericidal capacity (revealing changes in the viability of the particle-laden AMs). Since these four endpoints (or parameters) were visualized as four vectors, the in vitro assay was termed 'vector model'. The 'vector model' has been used to assess the in vitro effects of different materials relevant for the occupational setting [50, 57, 59].

In the present study, the concept of the 'vector model' was transferred to NR8383 cells, an AM cell line derived from rat lung lavage cells [60, 61]. Over many passages, NR8383 cells maintain their typical AM-like size, appearance, and phagocytic as well as immunological properties. They have been observed to react to test material exposure by the formation and release of different pro-inflammatory and fibrogenic cytokines and chemokines,

including TNF-α, IL-1, TGF-β and PDFG [60–65]. NR8383 cells have further been used to measure oxidative burst and ROS production as well as mitochondrial damage [61, 66]. On the gene expression level, different markers for oxidative damage, inducible nitric oxide synthase expression [64], inflammation, autophagy, and apoptotic balance were recorded in NR8383 cells [67].

Just as macrophages in general [68], NR8383 cells are more sensitive to test materials than e.g., lung epithelial cells [69]. NR8383 have been used for the in vitro testing of a variety of NMs including functionalized amorphous SiO$_2$, indium tin oxide, alumina, Al$_2$O$_3$, ultrafine TiO$_2$, (multi-walled) carbon nanotubes ((MW)CNTs), various copolymers and also heparin nanoparticles [64, 66, 69–75]. Generally, these studies differed with respect to fundamental aspects of the test protocol, such as medium composition, size of culture vessels, cell density, or incubation period. Furthermore, oftentimes well established materials serving as negative or positive controls (NCs, PCs) were not included. This, however, is a mandatory prerequisite for regulatory testing. It further forms an essential part of benchmark in vitro testing. Benchmark testing implies the comparative assessment of new materials against 'benchmark materials' which were previously tested and evaluated according to standard criteria. This benchmark testing is expected to constitute an important pillar in the safety assessment of the abundance of NM modifications available [21, 76].

In the present study, a test protocol was set up and applied that largely followed up on the testing strategy of the 'vector model' published by Bruch et al. [57, 77, 78], concordantly using non-nanosized corundum (Al$_2$O$_3$) and quartz DQ12 as NC and PC, respectively. Corundum was further used as negative (albeit micron-scaled) benchmark material, against which the in vitro test data were compared. The permanent NR8383 cells were selected as test system, and test materials were applied under protein-free cell culture conditions since protein supplementation of the culture medium has been observed to mitigate the in vitro cellular effects of NMs [21]. The selected endpoints comprised NM effects on membrane disruption and macrophage activation that were assessed by measuring cellular release of lactate dehydrogenase (LDH) and GLU. Pro-inflammatory reactions were assessed by measuring cellular release of bioactive TNF-α, and induction of oxidative stress was assessed by measuring the formation and release of H$_2$O$_2$.

Using this testing strategy, 18 inorganic NMs were assessed, covering metal oxides and sulphates (AlOOH, BaSO$_4$, CeO$_2$, Fe$_2$O$_3$, TiO$_2$, ZnO, and ZrO$_2$), precipitated, pyrogenic and colloidal amorphous SiO$_2$ and graphite nanoplatelets, and two nanosized organic pigments. CeO$_2$, ZrO$_2$ and colloidal amorphous SiO$_2$ were tested

Wiemann *et al. J Nanobiotechnol* (2016) 14:16

Page 4 of 27

without and with doping or surface functionalization. Thereby, the selected test materials covered a broad range of chemically different, but economically important nanosized materials.

The in vitro data collected performing the NR8383 AM assay evaluating LDH, GLU, TNF-α and H_2O_2 release were used to obtain an overview on the cellular effects of the altogether 20 test materials. Moreover, the present study was conceived to assess the applicability of the in vitro NR8383 AM assay within a tiered approach for regulatory NM hazard assessment. An example for such a tiered approach is the DF4nanoGrouping Decision-making framework for the grouping and testing of NMs put forward by Arts et al. [33, 79]. Within a tiered approach, the information gathered during the early non-animal tiers is used to determine whether higher tier in vivo testing is relevant for hazard assessment, or not.

Accordingly, it was assessed whether the data from the in vitro NR8383 assay allow recognizing passive NMs that will not elicit specific toxic effects upon inhalation exposure. If a NM can be assigned to the group of passive NMs based on the outcome of the in vitro NR8383 AM assay along with material and functional properties, in vivo inhalation studies may not be required for its hazard assessment. Further, it was assessed if the in vitro NR8383 AM assay allows identifying active NMs which elicit specific toxic effects upon inhalation exposure. Active NMs require further data and sub-grouping using in vivo inhalation testing to facilitate their hazard assessment.

Against this background, the in vitro data were used to develop a prediction model for the in vitro NR8383 AM assay that appeared best suited to distinguish passive from active NMs. As a 'gold standard' for the categorization of active and passive NMs, the findings from STISs (or sub-acute inhalation studies) available for all 20 test materials [10, 11, 58, 79–82] were used. A rat STIS no-observed-adverse-effect concentration (NOAEC) of <10 mg/m^3 was set as threshold value indicating NM activity, whereas NMs with STIS NOAECs of 10 mg/m^3 or higher were assessed as passive [33, 79]. Applicability of the in vitro NR8383 AM assay within a tiered approach for regulatory hazard assessment was evaluated by comparing the in vitro assignments of the test materials as either active or passive to the in vivo categorization.

Methods
Test materials
Ten of the altogether 18 inorganic NMs of the present study were used in the German Federal Ministry for Education and Research-funded projects NanoCare (i.e., AlOOH, BaSO$_4$ NM-220, nano-CeO$_2$, Al-doped CeO$_2$) and NanoGEM (i.e., ZrO$_2$.TODA, ZrO$_2$.acrylate, colloidal

SiO$_2$.naked (Levasil® 200) and its surface-functionalized variants SiO$_2$.PEG, SiO$_2$.amino, SiO$_2$.phosphate). Details on their physico-chemical characterization have been published by Driessen et al. [83], Kroll et al. [17], Kuhlbusch et al. [84], Hellack et al. [85], Izak-Nau and Voetz [86], and Landsiedel et al. [11].

Of these test materials, AlOOH (boehmite) was originally supplied by Sasol (Germany); BaSO$_4$ NM-220 by Solvay (Belgium); Al-doped CeO$_2$ by Evonik Industries AG (Germany); ZrO$_2$.TODA and ZrO$_2$.acrylate by itN Nanovation AG (Germany); SiO$_2$.naked by AkzoNobel AB (Sweden); and nano-CeO$_2$, SiO$_2$.PEG, SiO$_2$.amino, and SiO$_2$.phosphate by BASF SE (Germany).

Just as BaSO$_4$ NM-220, also six further NMs (i.e., TiO$_2$ NM-105, ZnO NM-111, precipitated SiO$_2$ NM-200 and pyrogenic SiO$_2$ NM-203, CeO$_2$ NM-211 and CeO$_2$ NM-212) were representative NMs of the OECD WPMN Sponsorship Programme for the Testing of Manufactured Nanomaterials. These six NMs were obtained from the EU Commission's Joint Research Centre (JRC, Ispra, Italy). Detailed characterization data for these OECD representative NMs have been published by Singh et al. [87, 88] and Rasmussen et al. [89, 90]. Of note, NM-x numberings (e.g., ZnO NM-110) refer to the respective codes of the OECD representative NMs (http://www. oecd.org/science/nanosafety/).

The inorganic red pigment Fe$_2$O$_3$ (hematite), the two nanosized organic pigments Diketopyrrololpyrrol (DPP) Orange N, and Pigment Blue 15:1 (Cu-phthalocyanin) and graphite nanoplatelets (GraphEx®) were provided by BASF SE, Germany (*cf.* Arts et al. [79] for extensive characterization data).

Finally, the micron-sized NC and benchmark material corundum (d$_{50}$: 2.2 μm) was purchased from ESK (Elektroschmelzwerk Kempten, Germany) and the micron-sized PC quartz dust DQ12 (d$_{50}$: 2.1 μm) from DMT GmbH & Co. KG (Germany).

Preparation of test material suspensions
All test materials were suspended in the cell culture medium (F-12K; Biochrom GmbH, Germany) and, for H_2O_2 determination, in Krebs-Ringer phosphate glucose (KRPG) buffer. KRPG buffer (pH value 7.3–7.4) is a physiological salt solution that contains 129 mM NaCl, 4.86 mM KCl, 1.22 mM CaCl$_2$, 15.8 mM NaH$_2$PO$_4$, and 5.5 mM glucose. In preparing the test material suspensions, approx. 1 mg of the dry-powder test items was weighed into a 15 mL polypropylene tube (Greiner, Germany). The necessary amount of fluid (3–10 mL) was added to achieve final maximum concentrations of 180 μg/mL F-12K medium or 360 μg/mL KRPG buffer, the latter being diluted twofold under testing conditions. Test items delivered as liquid suspensions (i.e.,

Wiemann *et al. J Nanobiotechnol* (2016) 14:16

Page 5 of 27

SiO₂.naked and its surface functionalized variants and both ZrO₂ NMs) were diluted accordingly. Upon suspension and/or dilution, the tubes were briefly vortexed to remove particles from the vessel wall. Afterwards, the preparations were ultrasonicated for 10 s using a probe adjusted to 50 W (Vibra Cell™, Sonics & Materials, USA). This step was recognized as indispensable to separate aggregates of the micron-scaled controls quartz DQ12 and corundum, and it was also included in preparing the dry-powder and liquid test items.

Due to poor dispersibility, the general protocol for test material preparation was adapted for the following test materials: SiO₂ NM-200 and NM-203, which were delivered strongly agglomerated, were treated with an ultrasonic probe on ice (5× for 1 min, each). Pigment Blue 15:1 and graphite nanoplatelets required pre-wetting in 0.5 % (v/v) ethanol. For this purpose, a stock dispersion of 2.56 mg/mL (with the further addition of 0.05 % (w/v) bovine serum albumin in the case of Pigment Blue 15:1 to warrant dispersion) was prepared by 10-min bath ultrasonication (Sonorex, DT106, Bandelin Electronic, Berlin, Germany). Fe₂O₃ and DPP Orange N were bath ultrasonicated (2× for 10 min, each) upon dispersion in double distilled water.

All test material suspensions were prepared shortly before in vitro application. For LDH, GLU and TNF-α determination, the suspensions were serially diluted with F-12K medium to achieve test concentrations of 22.5, 45, 90, and 180 µg/mL. For H₂O₂ determination, the test material suspensions were first diluted in KRPG buffer to a twofold of these concentrations (i.e., 45–360 µg/mL) since the Amplex red assay begins with a 1:1 dilution step (*cf.* "H₂O₂ formation" section). Accordingly, all four endpoints were generally assessed at final test material concentrations of 22.5-180 µg/mL. As exceptions from this rule, the highly bioactive ZnO NM-111 was tested for LDH and TNF-α at 2.8, 5.6, 11.2 and 22.5 µg/mL (but up to 180 µg/ml for GLU and H₂O₂). For technical reasons, ZrO₂.acrylate was assessed at 35–283 µg/mL. For all tests, material-free vehicle controls were carried out.

Particle size distribution in water, F-12K medium or KRPG buffer

The particle size distribution and agglomerating properties of the test materials suspended in water were assessed by particle tracking in the supernatant (detection range: 30–1000 nm) and by inspection of the agglomerates (detection range: >0.7 µm). All test material suspensions were diluted as necessary to achieve optimal measurement conditions of 5×10^8 particles/mL. Laser illumination combined with tracking analysis allowed detecting nanoparticles down to a concentration of 1×10^8/mL: The size distribution of the dispersed

particles was evaluated with a NanoSight LM 10 instrument (Malvern Instruments, England) equipped with a green (532 nm) or blue (405 nm) laser and using the accompanying NTA software 2.1–2.3. Agglomerated and gravitationally settled particles were recorded at the bottom of the culture vessels (96 well plates) using an inverted microscope (Axiocert 40C, Zeiss, Germany) equipped with phase contrast optics (10× or 20× objectives). Digital images (Axiocam C3, Zeiss, Germany) were taken after 16 h in the absence (cell-free controls) or presence of cells to document particle uptake under testing conditions [91].

Additionally, the test materials were analysed as described above suspended in 360 µg/mL KRPG buffer or 180 µg/mL F-12K medium. The incubation conditions were identical to the ones applied during in vitro testing, apart from the fact that no NR8383 cells were provided. Again, the suspensions were diluted as necessary to achieve optimal measurement conditions.

Preparation of the NR8383 test system

Rat NR8383 cells [60, 61] were originally purchased from ATCC (USA) and cultured in F-12K medium supplemented with 2 mM glutamine, penicillin/streptomycin (100 U/10 mg/mL; and 15 % (v/v) fetal calf serum (FCS; all from PAN Biotech GmbH, Germany). Cells were grown in 500 mL flasks (Greiner, Germany) under standard cell culture conditions (37 °C; 5 % CO₂) and passaged once a week. For the in vitro tests, cells were detached from the substrate by mechanical agitation, dispersed by pipetting, seeded into 96-well plates at 3×10^5 live cells per well and incubated in F-12K medium supplemented with 5 % FCS for 24 h. For test material application, supernatants were withdrawn, and test material-containing phenol red-free F-12K medium (Biochrom GmbH, Germany), supplemented with 2 mM glutamine and 100 U/100 µg/mL penicillin/streptomycin, was applied onto the cells. To correct for test material-specific adsorption and/or scattering of light, cell-free NM-containing controls were included in all test runs for all dilution steps. Cells were incubated with particles for 16 or 1.5 h. For the determination of LDH, GLU, and TNF-α release, cell culture supernatants were sampled after 16 h of incubation. In a parallel approach, supernatants were sampled after 1.5 h of incubation to assess H₂O₂ formation.

Lactate dehydrogenase and glucuronidase

To measure the amount of LDH and GLU released from the treated NR8383 cells, cell culture supernatants were harvested and centrifuged (10 min, 200 g) to remove cell debris. From each well, 50 µL was incubated with LDH reaction mix (Roche Cytotoxicity Kit; Roche, Germany) and evaluated as described by the manufacturer.

Wiemann *et al. J Nanobiotechnol (2016) 14:16*

Page 6 of 27

Measurements were corrected for cell free-adsorption and normalized to the PC value (set to 100 %) obtained from NR8383 cells lysed with 0.1 % Triton X-100 (Sigma Aldrich, Germany). To measure GLU activity, 50 μL of the supernatant was incubated at 37 °C with 100 μL 0.2 M sodium acetate buffer (pH 5) containing 13.3 mM p-nitrophenyl-D-glucuronide (Sigma Aldrich, Germany) and 0.1 % Triton X-100 [50]. The reaction was terminated after 2 h by addition of 100 μL 0.2 M NaOH (Merck KGaA, Germany). Optical density (OD) was measured at 405 nm in a plate photometer (Tecan 200Pro, Tecan, Germany); values were corrected for cell free-adsorption and normalized to the PC value (set to 100 %) again obtained from NR8383 cells lysed with 0.1 % Triton X-100.

Bioactive tumour necrosis factor alpha

To measure the bioactive TNF-α released from the treated NR8383 cells, cell culture supernatants were centrifuged and analysed using the L929 cytolysis test described by Desch et al. [92]. Briefly, 50 μL supernatant was pipetted onto 80 % confluent L929 mouse fibroblasts (ATCC, USA) in the presence of actinomycin D (Sigma Aldrich, Germany). After 24 h, the L929 cells were washed with phosphate buffered saline (PBS; Biochrom GmbH, Germany), stained with 0.5 % crystal violet (Sigma Aldrich, Germany), washed extensively with PBS, and lysed in an acidic mixture of citrate-buffered 50 % ethanol (Carl Roth GmbH, Germany). OD was measured at 570 nm, and results were expressed as L929 fibroblast lysis relative to non-treated medium controls, which were set to 0 %. Additionally, the L929 cells' responsiveness to TNF-α was controlled using a TNF-α standard (510-RT; Bio-Techne, Germany), and the uppermost value (1000 pg TNF-α/mL) was set to 100 %. As an additional PC, the TNF-α-forming capacity of NR8383 cells was confirmed by stimulation with lipopolysaccharide (LPS; 0.1 μg/mL, Sigma Aldrich, Germany). Finally, the direct effects of the test materials on L929 cells were assessed using 50 μL of the supernatants from cell-free NM-containing wells.

H$_2$O$_2$ formation

H$_2$O$_2$ synthesized by NR8383 cells and released into the supernatant was quantified in the Amplex red assay by measuring the formation of resorufin. All chemicals used within this assay were supplied by Sigma Aldrich (Germany). NR8383 cells were seeded in 96-well microtitre plates at a density of 3×10^5 cells/well and incubated under standard cell culture conditions. After 24 h, the medium was replaced by 100 μL of the test materials suspended in KRPG buffer. Immediately after incubation with the test material suspensions, 100 μL/well of a freshly prepared reaction mix containing 0.1 mM

Ampliflu, 2 mM NaN$_3$, and 2 U/mL horseradish peroxidase was added and incubated at 37 °C for 90 min. KRPG buffer was used as NC and 180 μg/mL zymosan as PC. Accuracy of the reactions was controlled with a 30 μM H$_2$O$_2$ standard concentration prepared from a 30 % stock solution freshly prepared from a 30 % H$_2$O$_2$ stock solution. OD was measured at 570 nm and 620 nm (reference value), corrected for background absorbance of cell free-particle controls and converted into absolute concentrations of H$_2$O$_2$ using the molar extinction coefficient of resorufin (54,000 L $\times$ mol^{-1} $\times$ cm^{-1}).

Statistical analysis

In vitro data were generated in triplicates and at least three independent repetitions were carried out. Data were expressed as mean $\pm$ standard deviation (SD) and analysed with Graph Pad Prism software (Version 6; GraphPad Software Inc., USA). To test for significance, test values were compared to those from non-treated vehicle controls using 2-way ANOVA and Dunnett's post hoc multiple comparison test. Test results with p $\leq$ 0.05 were assessed as significant (*). Additionally, the significance of results was assessed by comparison to the effects elicited by equal particle concentrations of the negative benchmark material corundum. Finally, the concordance of the in vitro NR8383 AM assay results and the outcome of in vivo inhalation studies was assessed using Cooper statistics [93].

Prediction model

A prediction model was developed to enable using the data from the in vitro NR8383 AM assay to distinguish active from passive NMs.

Test material categorization as 'active' or 'passive' using STIS data

The primary ('gold standard') distinction between active and passive (nano)materials was based upon in vivo rat STIS data that were available for the test materials [10, 11, 79–82]. Only for AlOOH, the available in vivo inhalation data were not recorded after 5-day inhalation exposure to rats (i.e., following the STIS test protocol), but in a 28-day sub-acute inhalation study conducted in accordance with OECD TG 412 [58].

NOAECs < 10 mg/m^3 that were assigned on account of any adverse treatment-related inflammatory reaction elicited in the rat upon 5-day inhalation exposure of the given NM under the testing conditions of the well-defined STIS resulted in test material assignment as active. This definition considered any inflammatory effect recorded by haematology, BALF evaluation, and/or lung histopathology. Test materials were assigned as passive if no treatment-related findings were recorded at 10 mg/m^3

Wiemann *et al. J Nanobiotechnol (2016) 14:16*

Page 7 of 27

or even higher concentratons in the STIS. Accordingly, their NOAEC was 10 mg/m^3 or higher (indicated as '≥' in Table 3). Since AlOOH was tested for 28 days (i.e., for four consecutive 5-day exposure periods), the NOAEC that Pauluhn [58] recorded for this material (i.e., 3 mg/m^3) was converted to a 5-day NOAEC by multiplying it by a factor of four (i.e., 12 mg/m^3) [94].

The recorded STIS NOAECs and lowest-observed-adverse-effect concentrations (LOAECs) for those materials that elicited inflammatory effects in at least one test group are provided in Table 3. Based thereupon, quartz DQ12, TiO$_2$ NM-105, ZnO NM-111, all CeO$_2$ test materials, as well as the three SiO$_2$ NMs without surface functionalization (i.e., SiO$_2$.naked, SiO$_2$ NM-200 and NM-203) were categorized as in vivo active, and all other test materials were categorized as in vivo passive (*cf.* "In vitro studies and test material assignment as active or passive" section for further details on the available in vivo data). The prediction model for the in vitro NR8383 AM assay was conceived to provide the best possible correlation to this in vivo categorization.

Determination of in vitro lowest-observed effect concentration

The data obtained for all four in vitro endpoints (or 'parameters', i.e., LDH, GLU, TNF-α, H$_2$O$_2$) were recorded separately for all test materials. As described in "Statistical analysis" section, the significance of individual test results was assessed by comparing them both to the results obtained for the non-treated cell controls (Table 3) and the negative benchmark material corundum (Additional file 1: Table S1). The lowest dose at which significant effects were recorded for a given endpoint-specific test result was termed in vitro LOAEC.

Definition of in vitro threshold value

Consistent with the 'vector model' described by Rehn et al. [54, 55], in which the in vitro dosages were set to cover the mass-based in vivo concentration range that is likely to be taken up by rat AMs (*cf.* "Background" section), a mass-based dose metric was primarily used both for the in vitro testing and to assess the in vivo STIS findings. However, the effects of NMs on AMs may not be directly related to the particle mass. While the dose metric of particle volume appears relevant to determine AM overloading [23, 24], at test material concentrations below the threshold for volume overload, the effects of NMs on AMs appear to be mainly conveyed by the particle surface. Accordingly, surface area has been suggested as a more appropriate dose metric for the in vitro testing of NMs [95–99].

To convert the mass-based test material concentrations into surface area-based concentrations, the applied mass concentrations (μg/mL) were multiplied with the respective test material's surface area (m^2/g) as assessed by the method of Brunauer Teller and Emmett (BET). The BET surface area is an approximation of the actual surface area of primary particles and/or agglomerates to the biologically accessible surface [100]. This conversion resulted in the dose metric of particle surface area per volume (mm^2/mL).

For the in vitro distinction between active and passive test materials, a threshold value of 4000 μm^2 per NR8383 cell (mean diameter: 12.5 μm) was set at the cellular level (see also "Test protocol, prediction model, and threshold values" section for explanation). This value corresponds to 1200 mm^2 particle surface area per 3 × 10^5 cells which actively gather particles at the bottom of a well of a 96-well culture plate (equivalent to 3600 mm^2/cm^2 cell culture surface area). As the cell culture wells are filled with 200 μL culture medium the above threshold value amounts to 6000 mm^2/mL and this dimension was used to convert applied test material concentrations (expressed in μg/mL) into the in vitro LOAEC values as shown in Table 3. Any significant in vitro LOAEC recorded below this threshold value was interpreted as biologically relevant, i.e., NM-specific cellular effect. By contrast, a significant in vitro LOAEC that was only recorded at a test material concentration exceeding the threshold was interpreted as unspecific and being caused by cellular overload, but not by particle-specific toxicity.

In vitro definition of 'active' and 'passive' test materials

To strengthen the robustness of the assay and to rule out incidental or borderline reactions by founding assignments on one affected endpoint alone, NMs were only assigned as active if significant in vitro LOAECs below the threshold value of 6000 mm^2/mL were recorded for at least two of the four in vitro endpoints (e.g., elevated LDH and TNF-α). The occurrence of no or only one significant in vitro LOAEC below the threshold value of 6000 mm^2/mL resulted in NM assignment as passive. (Nevertheless, the occurrence of one significant finding alone may be noteworthy for the further investigation of specific mechanisms of toxicity.)

Results

Test material characterization

Table 1 presents the test materials' primary particle size (PPS; determined by transmission electron microscopy (TEM) or scanning electron microscopy (SEM)), BET surface area, and their particle size distribution (mean or modal values, d$_{50}$ and d$_{90}$) in water, KRPG buffer or F-12K medium. In general, particle sizes measured with tracking analysis in H$_2$O were larger than the corresponding PPS. This was assessed as being either an indication for

Wiemann *et al. J Nanobiotechnol* (2016) 14:16

Page 8 of 27

Table 1 Primary characterisation of the test materials and agglomeration in biological fluids

Test materials	Size SEM, TEM [nm]	Surface area BET [m²/g]	Form	Size in H₂O [nm]	Size in KRPG [nm]	Size in F-12 K [nm]	Conc. in F-12K [Particles/mL]
TiO_2 NM-105	28	47	P	d_{50} 167 d_{90} 246	Not detectable	Not detectable	Not detectable
ZnO NM-111	82	15	P	Not detectable	Not detectable	Not detectable	Not detectable
Nano-CeO_2	40	33	P	d_{50} 159 d_{90} 263	Not detectable	Not detectable	Not detectable
Al-doped CeO_2	2–160	46	P	d_{50} 132 d_{90} 189	Not detectable	Not detectable	Not detectable
CeO_2 NM-211	10–20	66	P	d_{50} 130 d_{90} 199	Not detectable	Not detectable	Not detectable
CeO_2 NM-212	10–20	27	P	d_{50} 136 d_{90} 195	Not detectable	Not detectable	Not detectable
SiO_2.naked	5–50	200	S	d_{50} 48 d_{90} 91	d_{50} 58 d_{90} 99	d_{50} 59 d_{90} 94	2.3×10^{11}
SiO_2.PEG	8–45	200	S	d_{50} 54 d_{90} 83	Not detectable	Not detectable	Not detectable
SiO_2.amino	5–50	200	S	d_{50} 50 d_{90} 75	d_{50} 90 d_{90} 148	d_{50} 72 d_{90} 120	2.9×10^{11}
SiO_2.phosphate	5–50	200	S	d_{50} 52 d_{90} 83	d_{50} 67 d_{90} 107	d_{50} 68 d_{90} 106	1.0×10^{11}
SiO_2 NM-200	10–20	189	P	d_{50} 129 d_{90} 177	Not detectable	Not detectable	Not detectable
SiO_2 NM-203	5–30	200	P	d_{50} 151 d_{90} 210	d_{50} 174 d_{90} 305	Not detectable	Not detectable
AlOOH	40	47	P	d_{50} 163 d_{90} 243	Not detectable	Not detectable	Not detectable
$BaSO_4$ NM-220	25	41	P	d_{50} 86 d_{90} 130	Not detectable	Not detectable	Not detectable
Fe_2O_3 (hematite)	15	98	P	d_{50} 88 d_{90} 159	d_{50} 64 d_{90} 142	d_{50} 113 d_{90} 328	2.7×10^8
ZrO_2.TODA	3–15	117	S	d_{50} 77 d_{90} 113	Not detectable	Not detectable	Not detectable
ZrO_2.acrylate	9	117	S	d_{50} 172 d_{90} 244	Not detectable	Not detectable	Not detectable
DPP orange N	30–400 × 10–50	64	P	d_{50} 108 d_{90} 179	d_{50} 129 d_{90} 183	d_{50} 89 d_{90} 230	1.3×10^8
Pigment blue 15:1	17	53	P	d_{50} 191 d_{90} 293	d_{50} 193 d_{90} 290	d_{50} 173 d_{90} 263	2.1×10^9
Graphite nanoplatelets	<30 μm (flakes)	74	P	Not detectable	Not detectable	Not detectable	Not detectable

Primary particle size and BET surface area values were taken from Landsiedel et al. [11], Kroll et al. [17], Singh et al. [87, 88], and Rasmussen et al. [89, 90]

Form of the as-supplied test materials: Powder (P); Suspension (S)

Size measurements of the NM preparationss were carried out with NanoSight tracking analysis in double destilled water, in KRPG buffer, and F-12K culture medium; not detectable: not detectable due to low or missing particle concentration

Conc.: Concentration of nanoparticles as indicated by the NanoSight software; values were multiplied by the dilution factor

agglomeration and/or the material-dependent detection limit of the tracking analysis method.

For most test materials, the numbers of particles dispersed in KRPG buffer or F-12K medium after 16-h incubation underscored the detection limit for reliable tracking analysis (indicated as 'not detectable' in Table 1). Only for SiO_2.naked, SiO_2.amino, SiO_2.phosphate, SiO_2 NM-203, the inorganic pigment Fe_2O_3, and the two organic pigments DPP Orange N and Pigment Blue

15:1, measurable numbers of dispersed particles were recorded in KRPG buffer or F-12K medium at the end of the incubation period (Table 1):

Despite their small size and low light scattering properties, colloidal SiO_2.naked and its negatively charged surface functionalized variants SiO_2.amino and SiO_2. phosphate were observable with tracking analysis in H_2O, and particle sizes matched the upper PPS. Under testing conditions, i.e., in KRPG buffer and in F-12K medium,

Wiemann *et al. J Nanobiotechnol* (2016) 14:16

Page 9 of 27

particle sizes of these materials only slightly increased, gravitational settling was minimal, and only few agglomerates became visible at the bottom of the culture dish. Particle concentrations in F-12K medium ranged from 1.0×10^{11} particles/mL for SiO_2.phosphate to 2.9×10^{11} particles/mL for SiO_2.amino. By contrast, the neutral SiO_2.PEG completely agglomerated in all media and no dispersed nanoparticles were detectable in either KRPG buffer or F-12K medium.

Unlike the colloidal SiO_2 NMs, the dry-powder amorphous SiO_2, i.e., precipitated SiO_2 NM-200 and pyrogenic SiO_2 NM-203, required extensive ultrasonication to destroy large agglomerates. Nevertheless, dispersed SiO_2 NM-200 or NM-203 nanoparticles were not detectable by tracking analysis in F-12K medium at the end of the incubation period (but in KRPG buffer for SiO_2 NM-203). For both dry-powder SiO_2 test items, gravitational settling occurred that was more pronounced than for the colloidal SiO_2 NMs.

Within 16 h, low, but detectable amounts of dispersed particles of inorganic Fe_2O_3 or organic DPP Orange N were observed in the F-12K supernatant with mean particle sizes of 113 and 89 nm, respectively. By comparison, the PPSs were 15 nm for Fe_2O_3 and $30–400 \times 10–50$ nm for DPP Orange N. Even though slight colourations remained in the medium after agglomerate sedimentation, this could be corrected for using cell-free controls and, therefore, did not affect the OD measurements. Particle concentrations in F-12K medium were 2.7×10^8 for Fe_2O_3 and 1.3×10^8 for DPP Orange N, i.e., by a factor of 10^3 lower than the concentrations recorded for the dispersed colloidal SiO_2 NMs.

Pigment Blue 15:1 could be dispersed in H_2O by ultrasonication (180 µg/mL resulted in 5×10^{10} particles/mL; d_{50}:191 nm as compared to a PPS of 17 nm). However, less than 5 % of that particle number concentration were observed in F-12K medium after 16 h incubation (180 µg/mL resulted in 2.1×10^9 particles/mL; d_{50}: 173 nm) in spite of the addition of 0.05 % (w/v) bovine serum albumin during ultrasonication. The vast majority of this nanosized pigment formed blue agglomerates.

Cellular uptake of the test materials

Agglomerated particles settled to the bottom of the culture vessel where they were visible with phase contrast optics. As a rule, the test materials agglomerated and settled gravitationally within the 16-h incubation period. This settling occurred within minutes for corundum, within less than 1 h for quartz DQ12, 3–4 h for ZrO_2. TODA, 6 h for ZrO_2.acrylate, or by the end of the 16 h incubation period for TiO_2 NM-105 and all four CeO_2 NMs. Further as a rule, up to the highest test material concentration of 180 µg/mL, all test materials were completely engulfed by the NR8383 AMs (that are present at the bottom of the cell culture vessels) by the end of the 16-h incubation period (*cf.* Fig. 1 for phase-contrast images of settled particles and test material-laden NR8383 AMs for corundum, quartz DQ12, TiO_2 NM-105, CeO_2 NM-212, SiO_2.naked, $BaSO_4$ NM-220, DPP Orange N, and graphite nanoplatelets).

As exceptions to this rule, additional and specific observations were made for the following materials. Whereas complete cellular uptake was recorded for quartz DQ12 up to test concentrations of 90 µg/mL, many particles were visible outside deteriorated cells at 180 µg/mL underlining the pronounced cytotoxic effect of this material. AlOOH formed branched agglomerates under culture conditions which settled as a fluffy layer. For the different types of CeO_2 NMs, cellular uptake was complete up to a concentration of 90 µg/mL, whereas very few agglomerates remained between the NR8383 cells at 180 µg/mL. Graphite nanoplatelets have a strong light absorbance. Nevertheless this carbonaceous NM could be measured colourimetrically up to a concentration of 180 µg/mL since the substance precipitated. Although largely ingested by NR8383 macrophages, some large flocs of graphite nanoplatelets were not fully internalised, but were contacted by surrounding cells.

In conclusion, for most test materials, complete cellular uptake was recorded by the end of the incubation period at all tested concentrations. Only for SiO_2.naked, SiO_2.amino and SiO_2.phosphate, relevant proportions had not sedimented within 16 h (and hence could not be taken up by the AMs). Further, for graphene nanoplatelets, that did sediment, the highest test substance concentration was not fully internalized by the cells.

In vitro studies and test material assignment as active or passive

In the following, for each test material, the in vitro data are presented and evaluated to assign the material as either passive or active, and this in vitro assignment is directly compared to the outcome of the corresponding available in vivo studies and the resulting in vivo categorization as active or passive test materials.

Table 2 provides an overview of the data collected in the in vitro NR8383 AM assay determining extracellular release of LDH, GLU, TNF-α, and H_2O_2 listing all endpoint-specific data recorded at all test material concentrations (expressed in mass per volume metrics; i.e. µg/mL). In further processing these data, Table 3 presents the endpoint-specific significant in vitro LOAECs recorded for each test material, expressing these values both in mass per volume metrics and in relation to the BET surface area (i.e., mm^2/mL). Thereby, Table 3 reveals whether significant effects occurred below the threshold

Wiemann *et al. J Nanobiotechnol* (2016) 14:16
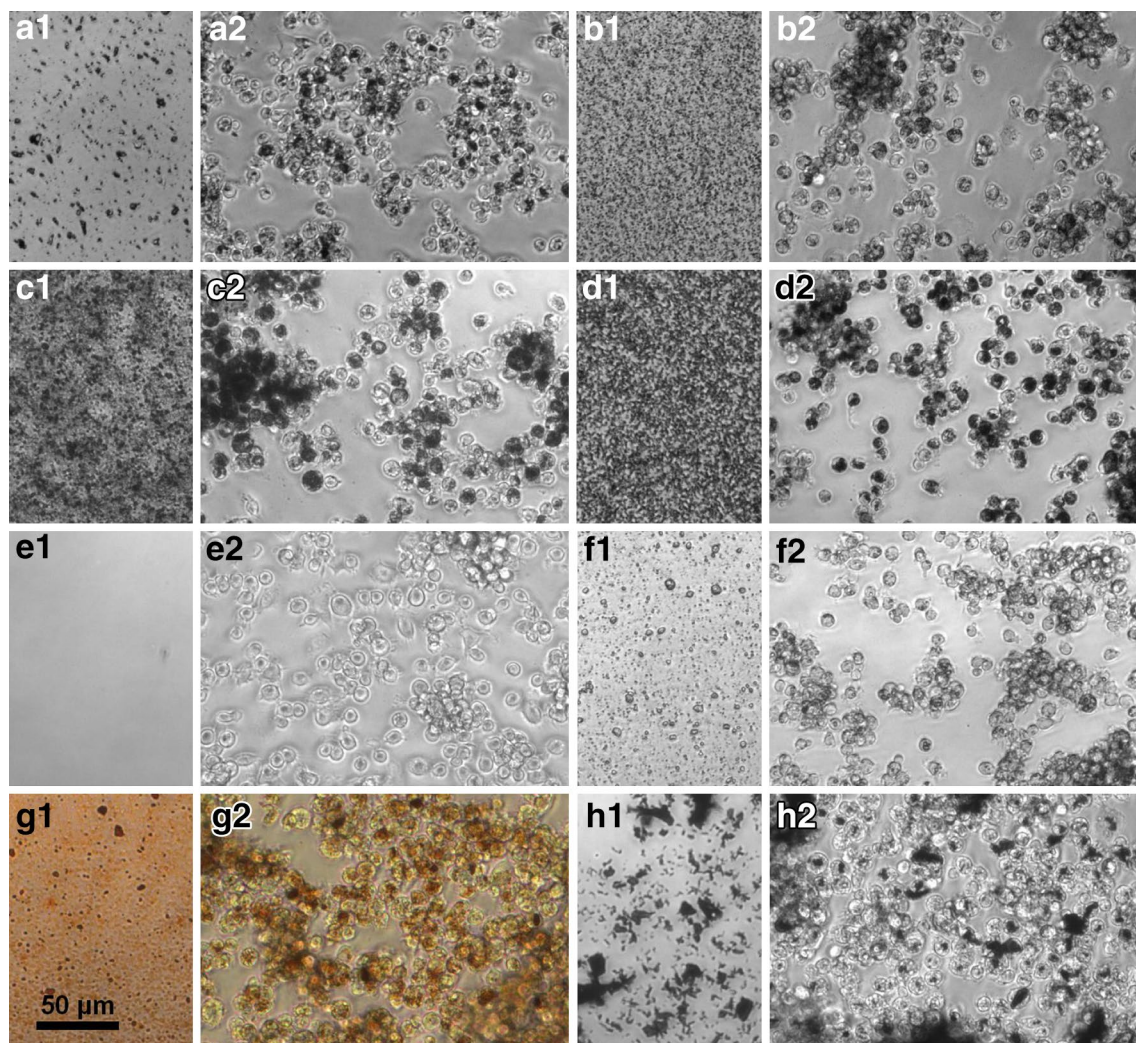
Page 10 of 27

Fig. 1 Test material sedimentation and uptake by NR8383 rat alveolar macrophages. A Corundum; B Quartz DQ12; C TiO₂ NM-105; D CeO₂ NM-212; E SiO₂.naked; F BaSO₄ NM-220; G DPP Orange N; H Graphite nanoplatelets. Phase contrast micrographs show settled particles at the bottom of cell-free wells in 96-well plates (**a1**–**h1** on the *left side* of the individual images) and corresponding particle-laden NR8383 cells at the end of the 16-h incubation period with the same particle concentration **a2**–**h2** on the *right side* of the individual images). Note that the uptake of particles (loaded with 90 μg/mL) appears complete as viewed by light microscopy, except for SiO₂.naked (loaded with 22.5 μg/mL), where settled particles are hardly visible

value of 6000 mm²/mL, and if so, how many parameters were significantly affected below the threshold for a given test material. Based thereupon, Table 3 further provides the in vitro NM assignments as either active or passive with contrasting juxtaposition to the STIS NOAECs, LOAECs and in vivo categorizations as active or passive.

For a better overview, Tables 2 and 3, just as the following subsections of "In vitro studies and test material assignment as active or passive", are subdivided into the following sections: First, the data for the NC and PC are provided, i.e., corundum (Al₂O₃) and quartz DQ12. Next, the data for the seven metal oxide NMs that were identified as active in vitro are presented, i.e., TiO₂ NM-105,

ZnO NM-111, and all four tested CeO₂ NMs. This is followed by the data recorded for the amorphous SiO₂ NMs. The subsequent section presents the data for the four metal oxide and metal sulphate NMs that were identified as passive in vitro, i.e., AlOOH, BaSO₄ NM-220, Fe₂O₃, and both surface-functionalized ZrO₂. The final two sections present the data recorded for the two nano-sized organic pigments and graphite nanoplatelets.

Corundum

In vitro, corundum is assigned as passive Corundum induced very slight dose-dependent increases of LDH, TNF-α and H₂O₂, all of which were not significantly dif-

Wiemann *et al. J Nanobiotechnol* (2016) 14:16

Page 11 of 27

Table 2 Effects of the negative control corundum, the positive control quartz DQ12, and the 20 test materials on the NR8383 cells

Test material	µg/mL	LDH [% of PC]	GLU [% of PC]	TNF-α [% standard][a]	ROS/H$_2$O$_2$ [% of PC]
Corundum	0	18.5 ± 2.7	3.7 ± 0.6	0.0 ± 0.0	2.7 ± 1.7
	22.5	17.3 ± 3.6	3.7 ± 0.6	14.3 ± 4.8	1.0 ± 0.3
	45	20.2 ± 3.1	4.2 ± 0.8	14.7 ± 5.7	1.4 ± 0.8
	90	23.2 ± 2.5	4.5 ± 0.2	16.5 ± 7.1	1.9 ± 0.9
	180	25.8 ± 2.5	4.7 ± 0.5	26.0 ± 5.1	2.2 ± 1.3
Quartz DQ12	0	20.5 ± 1.3	3.7 ± 0.6	0.0 ± 0.0	2.7 ± 1.7
	22.5	18.5 ± 2.6	4.2 ± 1.7	8.3 ± 5.1	3.6 ± 2.7
	45	31.3 ± 6.0	6.4 ± 1.5	47.6 ± 12.1*	3.4 ± 2.6
	90	66.4 ± 6.3*	15.0 ± 3.4*	80.9 ± 10.4*	4.6 ± 2.3
	180	95.4 ± 5.2*	31.7 ± 4.9*	95.8 ± 1.4*	5.7 ± 3.8
TiO$_2$ NM-105	0	18.0 ± 2.2	4.3 ± 3.5	0.0 ± 0.0	4.9 ± 4.3
	22.5	14.0 ± 2.9	3.5 ± 0.9	19.2 ± 17.2	4.9 ± 4.3
	45	26.2 ± 6.1	5.4 ± 1.7	25.8 ± 16.9	5.4 ± 4.9
	90	53.6 ± 5.9*	11.5 ± 1.7*	55.4 ± 7.6*	5.0 ± 3.1
	180	69.2 ± 1.1*	18.6 ± 0.7*	59.6 ± 6.6*	4.6 ± 4.8
ZnO NM-111[b]	0	27.4 ± 1.4	4.2 ± 2.5	0.0 ± 0.0	0.3 ± 0.2
	2.8/22.5	34.4 ± 1.4	4.1 ± 2.0	18.5 ± 5.0	0.0 ± 0.1
	5.6/45	36.7 ± 1.1*	7.7 ± 0.9	19.1 ± 0.5	0.3 ± 0.5
	11.3/90	39.1 ± 1.7*	18.2 ± 8.6*	13.2 ± 2.1	0.4 ± 0.6
	22.5/180	127.0 ± 2.7*	19.9 ± 4.6*	89.1 ± 1.4*	0.3 ± 0.7
nano-CeO$_2$	0	25.0 ± 2.9	5.2 ± 0.4	0.0 ± 0.0	1.3 ± 0.0
	22.5	18.5 ± 5.1	4.2 ± 0.2	20.5 ± 9.8	1.3 ± 0.2
	45	28.4 ± 3.3	4.5 ± 0.1	35.8 ± 23.9*	1.2 ± 0.5
	90	45.1 ± 2.1*	5.4 ± 0.2	89.3 ± 10.6*	2.8 ± 1.0
	180	74.3 ± 9.3*	9.8 ± 0.5*	96.2 ± 5.3*	4.7 ± 1.1
Al-doped CeO$_2$	0	25.0 ± 2.9	5.2 ± 0.4	0.0 ± 0.0	1.3 ± 0.0
	22.5	26.0 ± 8.4	5.0 ± 0.1	64.9 ± 35.2*	3.1 ± 0.1
	45	56.5 ± 11.2*	8.6 ± 0.8	84.7 ± 14.1*	3.2 ± 0.5
	90	84.1 ± 15.0*	19.8 ± 1.3*	89.8 ± 9.9*	4.2 ± 1.5
	180	91.1 ± 14.7*	25.0 ± 0.3*	88.4 ± 12.6*	5.7 ± 0.5
CeO$_2$ NM-211	0	25.0 ± 2.9	5.2 ± 0.4	0.0 ± 0.0	1.3 ± 0.0
	22.5	26.5 ± 8.5	6.0 ± 0.1	70.8 ± 11.1*	0.6 ± 0.9
	45	38.9 ± 7.8	5.7 ± 0.2	65.4 ± 13.3*	0.3 ± 0.7
	90	56.5 ± 7.0*	6.7 ± 0.2	75.0 ± 17.2*	2.7 ± 1.2
	180	75.0 ± 7.1*	9.9 ± 0.1*	85.6 ± 15.6*	4.4 ± 1.7
CeO$_2$ NM-212	0	25.0 ± 2.9	5.2 ± 0.4	0.0 ± 0.0	1.3 ± 0.0
	22.5	17.9 ± 7.8	4.9 ± 0.4	63.8 ± 29.4*	1.8 ± 0.8
	45	29.2 ± 12.0	6.0 ± 2.2	66.7 ± 26.3*	1.1 ± 2.1
	90	45.7 ± 14.6*	5.4 ± 0.2	76.9 ± 22.0*	2.9 ± 0.2
	180	69.0 ± 16.6*	9.9 ± 0.8*	88.5 ± 10.7*	1.8 ± 0.5
SiO$_2$.naked	0	19.9 ± 1.2	2.7 ± 2.0	0.0 ± 0.0	3.7 ± 2.1
	22.5	40.5 ± 2.6*	5.0 ± 1.2	79.6 ± 3.0*	4.6 ± 2.9
	45	87.6 ± 9.8*	14.7 ± 3.7*	93.4 ± 5.7*	10.7 ± 3.8*
	90	100.1 ± 5.8*	24.6 ± 4.5*	77.3 ± 30.7*	13.9 ± 1.6*
	180	83.8 ± 19.0*	25.8 ± 3.7*	65.0 ± 33.2*	14.1 ± 2.3*

Wiemann *et al. J Nanobiotechnol (2016) 14:16*

Page 12 of 27

Table 2 continued

Test material	µg/mL	LDH [% of PC]	GLU [% of PC]	TNF-α [% standard][a]	ROS/H$_2$O$_2$ [% of PC]
SiO$_2$.PEG	0	19.9 ± 1.2	2.7 ± 2.0	0.0 ± 0.0	3.7 ± 2.1
	22.5	22.8 ± 5.2	3.1 ± 0.6	26.2 ± 0.9	1.5 ± 4.3
	45	30.5 ± 7.0	3.5 ± 1.1	26.2 ± 2.4	6.7 ± 4.1
	90	69.9 ± 7.9*	10.8 ± 2.4*	61.6 ± 6.4*	10.2 ± 5.7
	180	87.8 ± 7.8*	24.4 ± 4.5*	91.2 ± 4.4*	14.6 ± 6.8*
SiO$_2$.amino	0	19.9 ± 1.2	2.7 ± 2.0	0.0 ± 0.0	3.7 ± 2.1
	22.5	22.0 ± 1.8	3.0 ± 0.5	44.4 ± 3.8*	4.4 ± 1.8
	45	70.4 ± 2.3*	8.2 ± 1.5*	99.1 ± 1.1*	5.5 ± 3.0
	90	96.2 ± 13.1*	17.9 ± 5.4*	99.1 ± 1.1*	6.6 ± 3.5
	180	99.7 ± 12.2*	25.8 ± 8.4*	98.3 ± 0.8*	13.0 ± 6.8*
SiO$_2$.phosphate	0	19.9 ± 1.2	2.7 ± 2.0	0.0 ± 0.0	3.7 ± 2.1
	22.5	16.6 ± 2.5	2.3 ± 0.5	25.0 ± 4.9	10.1 ± 4.2
	45	29.8 ± 12.5	3.1 ± 0.3	19.9 ± 5.1	25.4 ± 6.2*
	90	41.7 ± 21.7*	4.8 ± 1.4	53.0 ± 24.7*	37.2 ± 8.1*
	180	48.6 ± 22.1*	7.3 ± 5.0*	78.7 ± 8.8*	36.8 ± 6.4*
SiO$_2$ NM-200	0	13.2 ± 1.2	4.8 ± 3.1	0.0 ± 0.0	0.4 ± 0.2
	22.5	61.0 ± 2.1*	14.0 ± 5.6*	34.2 ± 25.0*	0.5 ± 1.5
	45	90.8 ± 18.7*	26.6 ± 9.1*	46.2 ± 21.4*	0.5 ± 1.0
	90	94.9 ± 13.8*	30.0 ± 4.8*	61.3 ± 22.6*	0.4 ± 1.0
	180	88.2 ± 15.0*	23.5 ± 7.2*	72.0 ± 18.6*	0.3 ± 1.1
SiO$_2$ NM-203	0	13.2 ± 1.2	4.8 ± 3.1	0.0 ± 0.0	0.4 ± 0.2
	22.5	83.9 ± 23.6	33.7 ± 6.4*	50.2 ± 16.7	0.7 ± 1.1
	45	88.1 ± 13.8	34.3 ± 5.1*	49.8 ± 14.2	0.7 ± 1.2
	90	85.3 ± 16.3*	30.1 ± 8.7*	50.0 ± 18.3	0.5 ± 0.8
	180	86.7 ± 16.2*	32.2 ± 5.7*	64.4 ± 18.0*	0.3 ± 0.7
AlOOH	0	20.5 ± 1.5	3.6 ± 0.1	0.0 ± 0.0	0.3 ± 0.1
	22.5	20.7 ± 1.6	3.5 ± 0.1	5.2 ± 0.3	0.0 ± 0.0
	45	22.7 ± 1.6	3.3 ± 0.1	13.4 ± 1.8	0.0 ± 0.0
	90	39.9 ± 0.1*	4.4 ± 0.1	14.8 ± 0.2	0.2 ± 0.3
	180	61.5 ± 0.4*	6.6 ± 0.2	37.6 ± 4.1*	0.2 ± 0.2
BaSO$_4$ NM-220	0	22.2 ± 0.9	3.0 ± 0.3	0.0 ± 0.0	1.8 ± 2.0
	22.5	24.0 ± 3.0	4.0 ± 0.3	0.0 ± 0.0	1.8 ± 2.1
	45	27.5 ± 3.3	3.6 ± 0.4	0.0 ± 0.0	1.8 ± 2.4
	90	30.2 ± 4.6	3.8 ± 0.3	0.0 ± 0.0	1.7 ± 2.0
	180	37.1 ± 5.9	3.8 ± 0.4	2.5 ± 0.1	1.7 ± 1.8
Fe$_2$O$_3$ (hematite)	0	22.1 ± 1.9	1.2 ± 1.0	0.0 ± 0.0	2.0 ± 0.8
	22.5	20.0 ± 0.6	1.6 ± 0.7	17.5 ± 4.2	3.1 ± 0.6
	45	25.4 ± 5.4	2.1 ± 0.5	16.5 ± 0.4	3.5 ± 0.4
	90	26.0 ± 0.6	2.2 ± 0.4	32.1 ± 10.3*	4.1 ± 0.6
	180	25.6 ± 0.9	2.8 ± 0.5	64.3 ± 33.2*	4.0 ± 1.0
ZrO$_2$.TODA	0	22.7 ± 3.5	2.8 ± 2.1	0.0 ± 0.0	1.1 ± 0.6
	22.5	25.7 ± 3.5	2.9 ± 1.1	21.8 ± 3.9	1.8 ± 0.5
	45	39.9 ± 7.9*	3.0 ± 1.1	21.8 ± 6.4	5.8 ± 1.6
	90	70.2 ± 8.4*	5.4 ± 0.8	68.7 ± 15.5*	8.3 ± 1.4*
	180	81.2 ± 12.8*	7.2 ± 0.2	87.9 ± 10.5*	8.0 ± 2.3*

Wiemann *et al. J Nanobiotechnol (2016) 14:16*

Page 13 of 27

Table 2 continued

Test material	µg/mL	LDH [% of PC]	GLU [% of PC]	TNF-α [% standard]ᵃ	ROS/H₂O₂ [% of PC]
ZrO₂.acrylateᶜ	0	22.7 ± 3.5	2.8 ± 2.1	0.0 ± 0.0	1.1 ± 0.6
	35	29.6 ± 8.4	3.3 ± 1.2	25.3 ± 4.7	0.7 ± 2.1
	70.5	49.0 ± 13.6*	4.9 ± 1.6	48.5 ± 5.5*	7.4 ± 0.5
	141	73.9 ± 11.3*	11.7 ± 3.7*	90.5 ± 1.7*	15.2 ± 2.8*
	283	80.8 ± 4.1*	19.7 ± 5.8*	90.8 ± 6.2*	22.5 ± 4.7*
DPP orange N	0	22.1 ± 1.9	1.2 ± 1.0	0.0 ± 0.0	2.0 ± 0.8
	22.5	19.9 ± 1.9	1.8 ± 0.6	25.9 ± 16.5	1.0 ± 0.1
	45	22.7 ± 1.9	2.3 ± 0.6	48.7 ± 37.7*	1.5 ± 0.4
	90	25.7 ± 1.1	3.2 ± 0.4	66.0 ± 57.0*	2.2 ± 0.4
	180	28.4 ± 0.5	5.3 ± 0.7	81.5 ± 30.9*	3.3 ± 1.3
Pigment blue 15:1	0	20.5 ± 1.3	4.2 ± 0.2	Not determined	0.2 ± 0.2
	22.5	17.4 ± 3.1	6.0 ± 0.3		0.0 ± 0.0
	45	20.0 ± 3.6	8.4 ± 3.5		0.0 ± 0.0
	90	41.0 ± 7.2*	10.6 ± 0.6*		0.0 ± 0.0
	180	88.0 ± 7.9*	21.9 ± 2.2*		0.0 ± 0.0
Graphite nanoplatelets	0	22.1 ± 1.9	1.2 ± 1.0	0.0 ± 0.0	2.0 ± 0.8
	22.5	24.2 ± 2.6	2.6 ± 1.0	2.2 ± 2.9	1.4 ± 0.8
	45	26.3 ± 1.9	3.3 ± 1.2*	8.4 ± 4.8	2.1 ± 1.2
	90	29.9 ± 0.4	5.7 ± 1.9*	30.2 ± 17.2*	4.1 ± 2.0
	180	37.8 ± 3.3	11.8 ± 2.5*	74.8 ± 9.4*	7.1 ± 1.3

To test for significance, test values were compared to those from non-treated vehicle controls using 2-way ANOVA with Dunnett's post hoc multiple comparison test, and $p \leq 0.05$ was assessed as significant (*)

ᵃ Measurements of TNF-α are expressed as L929 fibroblast lysis relative to non-treated medium controls, which were set to 0 %

ᵇ Due to its high bioactivity, ZnO NM-111 was tested for release of LDH and TNF-α at 2.8–22.5 µg/mL, whereas GLU and H₂O₂ formation were assessed at 22.5–180 µg/mL

ᶜ For technical reasons, ZrO₂.acrylate was assessed at 35–283 µg/mL

ferent from the non-treated controls. This lack of effects confirms the suitability of corundum as NC and as a negative benchmark material.

In vivo categorization confirms corundum passivity Previous rat STISs underlined the inert nature of respirable corundum particles (aerosol concentration 20 mg/m³; 2-week exposure, 5 days/week; 5 h/day) [77]. Also in rat instillation studies, corundum proved to be a chemically inert particle which hardly elicited any pulmonary inflammatory or fibrogenic effects [101, 102]. However, high intratracheal instillation doses of 7.5 mg/rat lung [102] or 5 mg/100 g body weight [103], which are both in the overload range, elicited BALF changes that mainly consisted of elevated polymorphonuclear neutrophil (PMN) counts. In line with these findings, the United States National Institute for Occupational Safety and Health (NIOSH) has set an occupational exposure limit (OEL) of 5 mg/m³ for respirable corundum (summarized by Krewski et al. [104]). Taken together, corundum is categorized as passive in vivo, which confirms in vitro passivity.

Quartz DQ12

In vitro, quartz DQ12 is assigned as active The in vitro macrophage toxicity of quartz DQ12 is well-known [54, 105]. Quartz DQ12 induced dose-dependent releases of LDH, GLU, and TNF-α, significant well below the threshold value of 6000 mm²/mL. Even though quartz DQ12 hardly elicited any extracellular H₂O₂ formation, the findings confirm its suitability as PC and results in quartz DQ12 assignment as active material.

In vivo categorization confirms quartz DQ12 activity In a rat 28-day sub-acute inhalation study, a NOAEC of 0.1 mg/m³ was recorded for alpha-quartz (median particle size: 1.7 µm) [106]. Due to its progressive inflammatory, fibrogenic and genotoxic effects, micron-sized quartz DQ12 is widely used as a PC for in vivo studies [102, 107]. As PC, it was tested at one (high) concentration, each, in two rat 5-day STISs. At 25 mg/m³, quartz DQ12 produced progressively severe effects over the 3-month post-exposure period [80] with similar findings recorded at 100 mg/m³ [81]. Generally, the results observed in the

Wiemann *et al. J Nanobiotechnol* (2016) 14:16

Page 14 of 27

Table 3 Comparison of significant in vitro LOAECs to NOAECs and LOAECs recorded in rat short-term inhalation studies

Test materials		BET [m²/g]	In vitro NR8383 AM assay									STIS		Ref[d]
			LOAEC [µg/mL]				LOAEC [mm²/mL]					NOAEC [mg/m³]	LOAEC [mg/m³][a]	
Class	Name		LDH	GLU	TNF-α	ROS H₂O₂	LDH	GLU	TNF-α	ROS H₂O₂	Threshold <6000	Threshold <10		
Micron-sized crystalline silica	Quartz DQ12	8	90	90	45	n.s.	720	720	360	n.s.	3	0.1	1.0	[106]
Active metal oxide NMs	TiO₂ NM-105	47	90	90	90	n.s.	4230	4230	4230	n.s.	3	<2	2.0	[10]
	ZnO NM-111	15	5.6	90	22.5	n.s.	84	1350	338	n.s.	3	0.5	2.5	[11]
	nano-CeO₂	33	90	180	45	n.s.	2970	n.s.	1485	n.s.	2	0.5	2.5	[11]
	Al-doped CeO₂	46	45	90	22.5	n.s.	2070	4140	1035	n.s.	3	0.5	2.0	[11]
	CeO₂ NM-211	66	90	180	22.5	n.s.	5940	n.s.	1485	n.s.	2	<0.5	5.0	[111]
	CeO₂ NM-212	27	90	180	22.5	n.s.	2430	n.s.	608	n.s.	2	<0.5	5.0	[111]
Amorphous SiO₂ NMs	SiO₂ naked	200	22.5	45	22.5	45	4500	9000	4500	9000	2	2.5	10	[11]
	SiO₂ PEG	200	90	90	90	180	18000	18000	18000	36000	0	≥50	n.r.	[11]
	SiO₂ amino	200	45	45	22.5	180	9000	9000	4500	36000	1	≥50	n.r.	[11]
	SiO₂ phosphate	200	90	180	90	45	18000	n.s.	18000	9000	0	≥50	n.r.	[11]
	SiO₂ NM-200	189	22.5	22.5	22.5	n.s.	4253	4253	4253	n.s.	3	1	5	[80]
	SiO₂ NM-203	200	22.5	22.5	22.5	n.s.	4500	4500	4500	n.s.	3	1	5	[80]
Passive metal oxide and metal sulphate NMs	AlOOH	105	90	n.s.	180	n.s.	9450	n.s.	18900	n.s.	0	(3)[b]	(28)[b]	[58]
	BaSO₄	41	n.s.	n.s.	n.s.	n.s.	n.s.	n.s.	n.s.	n.s.	0	≥50	n.r.	[11]
	Fe₂O₃ (hematite)	98	n.s.	n.s.	90	n.s.	n.s.	n.s.	8266	n.s.	0	≥30	n.r.	[79]
	ZrO₂-TODA	117	45	n.s.	90	90	5265	n.s.	10530	10530	1	≥50	n.r.	[11]
	ZrO₂-acrylate	117	70.5	141	70.5	141	8249	16497	8249	16497	0	≥50	n.r.	[11]
Nanosized organic pigments	DPP Orange N	64	n.s.	n.s.	45	n.s.	n.s.	n.s.	2880	n.s.	1	≥30	n.r.	[79]
	Pigment Blue 15:1	53	90	90	n.d.[c]	n.s.	4770	4770	n.d.[c]	n.s.	2	≥30	n.r.	[79]
Carbonaceous NM	Graphite nanoplatelets	74	n.s	45	90	n.s	n.s	3330	6660	n.s	1	≥10	n.r.	[82]

For all parameters, the significant in vitro LOAECs (significance as compared to the vehicle controls) are shown, both in mass/volume (µg/mL) and surface area/volume (mm²/mL) dose metrics (n.s.: no significance). The surface area/volume-based values were calculated by multiplying the mass/volume values by the respective NM's BET surface area. Surface area/volume-based values that undercut the in vitro threshold of 6000 mm²/mL are provided in italics. For test material assignment as either active (significant LOAEC < 6000 mm²/mL, ≥ 2 of 4 parameters affected) or passive (0 or only 1 parameter affected), the frequency of affected parameters is indicated in the column 'threshold < 6000 mm²/mL'. Further, available rat STIS NOAEC values are provided for all test materials (and LOAEC values, if effects were observed). For both the in vitro and in vivo data, values indicating 'activity' are highlighted in bold italic

[a] n.r.: If no effects were observed in the STIS up to the highest tested concentration, no LOAEC was recorded (n.r.)

[b] Since AlOOH was tested for 28 days (i.e., four consecutive 5-day exposure periods), the NOAEC that Pauluhn [58] recorded for this material (i.e., 3 mg/m³) was converted to a 5-day NOAEC by multiplying it by a factor of four [94]. Accordingly, the calculated 5-day NOAEC of 12 mg/m³ indicates passivity

[c] For technical reasons, TNF-α was not determined (n.d.) for Pigment Blue 15:1. However, since significant in vitro LOAECs below the threshold were recorded for LDH and GLU, this does not impair its assignment as 'in vitro active'

[d] Numbers in brackets apply to (short-term) inhalation studies as listed in the reference section

Wiemann *et al. J Nanobiotechnol* (2016) 14:16

Page 15 of 27

STIS at the end of the post-exposure observation periods resembled those recorded in sub-chronic inhalation studies [108]: Macrophage, monocyte, PMN, and also lymphocyte counts were increased in the lung parenchyma and BALF, which coincided with elevated levels of total protein and enzyme activities [LDH, alkaline phosphatase (AP), γ-glutamyltransferase (GGT) and N-acetyl-glucosaminidase (NAG)]. Upon intratracheal instillation in rats, pulmonary fibrosis was observed even after bolus doses of only 0.15–0.3 mg [102, 109]. Such dosages may be reached under STIS conditions by aerosol concentrations that are far lower than 10 mg/m^3. In conclusion, quartz DQ12 is categorized as active material, which confirms the in vitro assignment.

Active metal oxide NMs (TiO$_2$, ZnO, CeO$_2$)

In vitro, TiO$_2$ NM-105 is assigned as active TiO$_2$ NM-105 elicited dose dependent increases of LDH, GLU, and TNF-α (significant in vitro LOAECs at 4230 mm^2/mL, each), whereas H$_2$O$_2$ formation did not differ from the vehicle control. Since significant in vitro LOAECs below the threshold value of 6000 mm^2/mL were recorded for 3 of the 4 parameters, TiO$_2$ NM-105 is assigned as active NM.

In vivo categorization confirms TiO$_2$ NM-105 activity In a number of different STISs assessing both coated and uncoated TiO$_2$ NMs, pulmonary inflammatory changes were recorded, with a NOAEC for TiO$_2$ NM-105 of <2 mg/m^3 and a LOAEC of 2 mg/m^3. Most prominent findings were BALF increases in total cell count, PMNs, and AMs. Additionally, total protein and the activities of LDH, ALP, GGT, NAG were increased [10, 11, 81]. Based upon these in vivo STIS data, TiO$_2$ NM-105 is categorized as active NM, which confirms the in vitro assignment.

ZnO NM-111 is assigned as in vitro active ZnO NM-111, that is coated with triethoxycaprylylsilane, is a NM with a comparably small BET surface area of 15.1 m^2/g. This material dissolves in acidic environments thereby shedding zinc ions [79]. Maximum cytotoxicity (release of LDH) was already observed at 22.5 μg/mL (significant in vitro LOAEC at 5.6 μg/mL, i.e., 84 mm^2/mL), while the parameter GLU became significant at 90 μg/mL (1350 mm^2/mL) and TNF-α induction was at its maximum between 22.5 and 45 μg/mL (in vitro LOAEC 338 mm^2/mL). TNF-α formation was inhibited at higher concentrations due to progressive cell degradation. Extracellular H$_2$O$_2$ formation induced by ZnO NM-111 was in the same range as the concurrent vehicle control value. In parallel studies, the non-coated core material ZnO NM-110 was even more toxic than coated ZnO NM-111 for all parameters tested

(data not shown). Since significant in vitro LOAECs below the threshold value of 6000 mm^2/mL were recorded for 3 of the 4 parameters, ZnO NM-111 (just as ZnO NM-110) is assigned as active NM.

In vivo categorization confirms ZnO NM-111 activity Coated ZnO NM-111 elicited extensive signs of inflammation in the BALF upon 5-day inhalation exposure to 2.5 mg/m^3 (NOAEC: 0.5 mg/m^3). The most prominent findings were increased total cell counts caused by invaded PMNs, lymphocytes, and monocytes [11]. Total protein concentration and enzyme activities (GGT, LDH, ALP and NAG) were increased as well, just as a number of inflammatory mediators, i.e., cytokine-induced neutrophil chemoattractant 1 (CINC-1, the rat homologue to IL-8), clusterin, cystatin C, granulocyte chemotactic protein 2 (GCP-2), and MCP-1. In a 14-day STIS, 8 mg/m^3 uncoated ZnO NM-110 (only this concentration tested) also elicited pulmonary inflammatory effects so that a 14-day NOAEC < 8 mg/m^3 was assigned to ZnO NM-110 [110]. Based upon these in vivo STIS data, ZnO NM-111 (just as ZnO NM-110) is categorized as active NM, which confirms the in vitro assignment.

All four CeO$_2$ NMs (Al-doped CeO$_2$, nano-CeO$_2$, CeO$_2$ NM-211, and CeO$_2$ NM-212) are assigned as in vitro active All four types of CeO$_2$ NMs dose-dependently increased LDH and GLU release. The in vitro LOAECs recorded for LDH were significant and below the threshold value of 6000 mm^2/mL for all four CeO$_2$ NMs. Additionally, for Al-doped CeO$_2$, the in vitro LOAEC recorded for GLU was significant and below the threshold value. Evaluation of these two parameters that indicate cell membrane damage resulted in the following ranking of cytotoxicity (when using the particle surface area-based LOAECs): Al-doped CeO$_2$ > CeO$_2$ NM-212 > nano-CeO$_2$ > CeO$_2$ NM-211. H$_2$O$_2$ formation was far less pronounced (and never significant), but also headed by Al-doped CeO$_2$. Finally, the in vitro LOAECs recorded for TNF-α induction were significant and below the 6000 mm^2/mL threshold value for all four CeO$_2$ NMs, albeit with a slightly different ranking, i.e., CeO$_2$ NM-212 > Al-doped CeO$_2$ > CeO$_2$ NM-211 = nano-CeO$_2$. Accordingly, the findings indicate different biological activities and potencies of in vitro cellular effects of the four tested CeO$_2$ NMs with Al-doped CeO$_2$ and CeO$_2$ NM-212 eliciting more pronounced effects than nano-CeO$_2$ or CeO$_2$ NM-211. Since significant in vitro LOAECs below the threshold value of 6000 mm^2/mL were consistently recorded for the two parameters LDH and TNF-α (and additionally for GLU in the case of Al-doped CeO$_2$), all four CeO$_2$ NMs are assigned as active.

Wiemann *et al. J Nanobiotechnol* (2016) 14:16

Page 16 of 27

In vivo categorization confirms activity for all four CeO$_2$ NMs   All four CeO$_2$ NMs induced a pronounced transient inflammation at 0.5 mg/m^3, and effects increased at higher doses up to 25 mg/m^3 [11, 111]. Three days post-exposure, relative PMN fractions in the BALF increased to 76 and 79 % for Al-doped CeO$_2$ and nano-CeO$_2$, respectively, and concomitantly, the BALF total protein levels were elevated [11]. For all four CeO$_2$ NMs, a NOAEC of <0.5 mg/m^3 was assigned [11, 111]. Accordingly, all four CeO$_2$ NMs are categorized as active, which confirms the in vitro assignment.

For an in-depth in vitro-in vivo comparison of the test results recorded for the four CeO$_2$ NMs, the in vitro data were further compared to specific BALF findings that are directly related to AM-induced alterations of the in vivo rat lung, i.e. absolute values of total cells, AM, PMN as well as total protein concentration. By contrast to the above-mentioned particle surface area-based in vitro ranking, the following ranking of cytotoxicity is achieved when using the mass-based in vitro data: Al-doped CeO$_2$ > CeO$_2$ NM-211 = nano-CeO$_2$ > CeO$_2$ NM-212. As presented in further detail in the Additional file 1: Table S2, the BALF findings [11, 111] allow the following conclusions on in vivo AM-related pulmonary alterations: Al-doped CeO$_2$ and nano-CeO$_2$ dose dependently decreased the number of AMs in the BALF and increased PMN counts and total protein concentration alike, whereas the corresponding effects elicited by CeO$_2$ NM-211 and CeO$_2$ NM-212 were approx. 60 % lower over the entire concentration range. Hence, even though the four different CeO$_2$ NMs were assigned the same STIS NOAEC of <0.5 mg/m^3, there were gradual differences in BALF parameters at nominally identical conditions of NM in the inspired air. Also the lung burdens recorded for the four different CeO$_2$ NMs upon 5-day inhalation exposure differed [11, 111]. These differences are partly reflected by the in vitro tests in which Al-doped CeO$_2$ was clearly more bioactive than e.g., CeO$_2$ NM-212, at least in the low to middle dose range.

Amorphous SiO$_2$ NMs

Colloidal SiO$_2$.naked is assigned as in vitro active and its surface-functionalized variants (SiO$_2$.PEG, SiO$_2$.amino, and SiO$_2$.phosphate) as in vitro passive   For all four colloidal SiO$_2$ NMs, significant in vitro LOAECs were recorded for all four test parameters with the exception of GLU for SiO$_2$.phosphate. However, as a rule, these significant LOAECs by far exceeded the threshold value of 6000 mm^2/mL. Only for SiO$_2$.naked, LDH and TNF-α attained 4500 mm^2/mL, each, and for SiO$_2$.amino, TNF-α attained this same value. Accordingly, only for the non-surface functionalized SiO$_2$.naked, two parameters with significant in vitro LOAECs below 6000 mm^2/mL, i.e., the

threshold for biologically relevant, particle-specific (i.e., non cellular overload-induced) effects, were recorded. In conclusion, SiO$_2$.naked is assigned as in vitro active, whereas its surface-functionalized variants SiO$_2$.PEG, SiO$_2$.amino, and SiO$_2$.phosphate are assigned as passive.

In vivo categorizations confirm both SiO$_2$.naked activity and the passivity of the surface-functionalized SiO$_2$ At 10 and 50 mg/m^3, SiO$_2$.naked evoked dose-dependent signs of inflammation in the rat STIS [11]. Three days after the final exposure, the most predominant significant effect in the BALF was an increased PMN count that was accompanied by slightly elevated BALF lymphocyte counts and moderately increased numbers of blood PMNs. In histopathological evaluation, multifocal macrophage aggregates were observed in the lung that exacerbated towards a slight multi-focal pulmonary inflammation by the end of the 3-week exposure free period. Accordingly, a NOAEC of 2.5 mg/m^3 was assigned to SiO$_2$.naked [11]. By contrast, no adverse effects were observed after inhalation exposure to up to 50 mg/m^3 SiO$_2$.PEG, SiO$_2$.phosphate, or SiO$_2$.amino, and the NOAEC for these materials was assessed as being ≥50 mg/m^3 [11]. Based upon the in vivo STIS data, SiO$_2$.naked is categorized as active NM and SiO$_2$.PEG, SiO$_2$.phosphate, and SiO$_2$.amino as passive NMs, which confirms the in vitro assignment.

SiO$_2$ NM-200 and NM-203 are assigned as in vitro active   Both precipitated SiO$_2$ NM-200 and pyrogenic SiO$_2$ NM-203 consistently elicited significant LDH, GLU and TNF-α release at 22.5 μg/mL, each. For all three parameters, this corresponds to significant in vitro LOAECs of 4253 and 4500 mm^2/mL, for SiO$_2$ NM-200 and NM-203, respectively. Accordingly, for both dry-powder amorphous SiO$_2$ NMs, two parameters, each, ranged below the threshold value of 6000 mm^2/mL, and both SiO$_2$ NM-200 and NM-203 are assigned as active.

In vivo categorization confirms SiO$_2$ NM-200 and NM-203 activity   For precipitated SiO$_2$ NM-200 and pyrogenic SiO$_2$ NM-203, STIS data were available for precipitated Zeosil® 45 and pyrogenic Cab-O-Sil® M5. The equivalence of these materials to SiO$_2$ NM-200 and NM-203, respectively, has been established based upon concordance in production process and minimum degree of material purity as well as comparability of specific surface area and agglomerate size [80, 112, 113]. In the rat STIS published by Arts et al. [80], test material concentrations of 1, 5, and 25 mg/m^3 were applied, and 1 mg/m^3 was recorded as NOAEC for both SiO$_2$ NM-200 and NM-203, whereas 5 mg/m^3 was assessed as LOAEC. For SiO$_2$ NM-200, increased weights of the lungs and lung-associated lymph nodes (LALNs) as well as an inflammatory response of

Wiemann *et al. J Nanobiotechnol (2016) 14:16*

Page 17 of 27

the lung tissue were recorded at 5 and 25 mg/m^3 that were accompanied by dose-dependently increased PMN counts, enzyme activities, and protein levels in the BALF. For SiO$_2$ NM-203, increased lung weights and hypertrophy of the bronchiolar epithelium were significant in the 5 and 25 mg/m^3 test groups. The LALNs contained increased silica levels, and, again, dose-dependently increased PMN and macrophage counts in the BALF indicated inflammatory reactions. For both materials, all effects were fully reversible within 3 months post-exposure [80]. Based upon the in vivo STIS data, SiO$_2$ NM-200 and NM-203 are categorized as active, which confirms the in vitro assignment.

Passive metal oxide and metal sulphate NMs (AlOOH, BaSO$_4$, Fe$_2$O$_3$, ZrO$_2$)

AlOOH is assigned as in vitro passive AlOOH (boehmite) elicited dose-dependent and significant increases of LDH and TNF-α (significant in vitro LOAECs: 9450 and 18,900 mm^2/mL, respectively). Hence, even though significant LOAECs were recorded for two parameters, both values ranged well above the threshold value of 6000 mm^2/mL indicating that the observed effects were elicited under in vitro cellular overload conditions. Accordingly, these effects are assessed as not-particle specific, and AlOOH is assigned as passive.

In vivo categorization confirms AlOOH passivity The AlOOH NM included in the present study (PPS: 40 nm; BET surface area: 105 m^2/g) and a smaller AlOOH variant (PPS: 10 nm; BET surface area: 182 m^2/g) were submitted to a 28-day rat sub-acute inhalation study followed by a 3-month post-exposure observation period [58]. In this study, no adverse effects were recorded at AlOOH aerosol concentrations of 0.4 or 3 mg/m^3. Pulmonary inflammation (recorded by significantly altered BALF parameters, increased lung and LALN weights and histopathological findings) was observed at 28 mg/m^3 AlOOH. However, these effects were only elicited by cumulative doses exceeding approx. 1 mg AlOOH/g lung at the end of the 28-day exposure period [58]. Since the concentration dependence and time-course changes of aluminum lung burden demonstrated a precipitous increase in elimination half-time at aerosol concentrations of 28 mg/m^3, Pauluhn assessed these findings as being consistent with pulmonary overload [58]. An earlier intratracheal instillation study confirmed these results indicating a NOAEC of 0.6 mg/rat lung, whereas reversible increases in BALF PMN and total protein levels were recorded at bolus doses of 1.2 mg/rat lung [84]. Since AlOOH was tested for 28 days (i.e., four consecutive 5-day exposure periods), the NOAEC of 3 mg/m^3 that Pauluhn [58] recorded for this

material was converted to a 5-day NOAEC by multiplying it by a factor of four [94]. In accordance with this calculated 5-day NOAEC of 12 mg/m^3, AlOOH is categorized as passive, which confirms the in vitro assignment.

BaSO$_4$ NM-220 is assigned as in vitro passive BaSO$_4$ NM-220 did not elicit any cellular effects that differed from the vehicle or corundum controls. Therefore, BaSO$_4$ NM-220 is assigned as passive.

In vivo categorization confirms BaSO$_4$ NM-220 passivity No adverse effects were observed in a rat STIS after inhalation exposure to up to 50 mg/m^3 BaSO$_4$ NM-220 [11]. Accordingly, BaSO$_4$ NM-220 is categorized as passive, which confirms the in vitro assignment.

Fe$_2$O$_3$ is assigned as in vitro passive For Fe$_2$O$_3$ (hematite), the only significant LOAEC was recorded for TNF-α (8266 mm^2/mL). This one in vitro LOAEC further exceeded the threshold value of 6000 mm^2/mL. Of note, the cytotoxic effects elicited by this nanosized Fe$_2$O$_3$ were equal to or lower than those of its bulk counterpart, whereas the amount of sedimented test material appeared comparable (data not shown). Since only one parameter was affected, nanosized Fe$_2$O$_3$ is assigned as passive.

In vivo categorization confirms Fe$_2$O$_3$ passivity Inhalation exposure to up to 30 mg/m^3 Fe$_2$O$_3$ (or its non-nanosized counterpart; data not shown) in a STIS did not cause any adverse effects in the rat lung as was determined by BALF evaluation, hematology and histopathological evaluation [79]. Based upon this in vivo study, Fe$_2$O$_3$ (just as its non-nanosized counterpart) is categorized as passive, which confirms the in vitro assignment.

ZrO$_2$.TODA and ZrO$_2$.acrylate are assigned as in vitro passive ZrO$_2$.TODA and ZrO$_2$.acrylate dose-dependently and significantly increased LDH, TNF-α, and H$_2$O$_2$ formation, and ZrO$_2$.acrylate additionally GLU. However, apart from the LDH value recorded for ZrO$_2$.TODA (in vitro LOAEC: 5265 mm^2/mL), which laid just below the 6000 mm^2/mL threshold, all other significant in vitro LOAECs recorded for either ZrO$_2$.TODA or ZrO$_2$. acrylate exceeded the threshold value. Accordingly, both ZrO$_2$.TODA and ZrO$_2$.acrylate are assigned as passive.

In vivo categorization confirms ZrO$_2$.TODA and ZrO$_2$. acrylate passivity No adverse effects were observed in a rat STIS after inhalation exposure to up to 50 mg/m^3 ZrO$_2$. acrylate or ZrO$_2$.TODA [11]. In rat intratracheal instillation studies, bolus dose-NOAECs of 0.6 and 1.2 mg/rat lung were recorded for ZrO$_2$.TODA and ZrO$_2$.acrylate,

Wiemann *et al. J Nanobiotechnol (2016) 14:16*

Page 18 of 27

respectively [114]. Based upon these in vivo studies, both ZrO_2.TODA and ZrO_2.acrylate are categorized as passive, which confirms the in vitro assignment.

Nanosized organic pigments

DPP Orange N is assigned as in vitro passive DPP Orange N elicited a significant increase of TNF-α (in vitro LOAEC 2880 mm²/mL) that ranged well below the threshold value of 6000 mm²/mL. However, since LDH, GLU, and H_2O_2 formation were not significantly altered, the premise that at least two of the four parameters had to be altered to indicate NM activity was not met. Of note, also the bulk counterpart to DPP Orange N, DPP Orange B, did not elicit relevant cytotoxicity in the in vitro NR8383 AM assay (data not shown). Accordingly, DPP Orange N (and DPP Orange B) are assigned as passive.

In vivo categorization confirms DPP Orange N passivity Inhalation exposure to up to 30 mg/m³ DPP Orange N in a STIS did not cause any adverse effects in the rat lung as was determined by BALF evaluation, hematology and histopathological evaluation [79]. For the respective bulk material DPP Orange B, high aerosol concentrations of 30 mg/m³ slightly increased total cell count, PMN, MCP-1 and osteopontin in the BALF (data not shown). Based upon these in vivo studies, DPP Orange N (just as DPP Orange B) are categorized as passive, which confirms the in vitro assignment.

Pigment Blue 15:1 is assigned as in vitro active Pigment Blue 15:1 elicited dose-dependent increases of LDH and GLU with significant LOAECs of 4770 mm²/mL, each. (The slightly blue colouration of the supernatants could be corrected for via cell-free controls.) Accordingly, two parameters had significant LOAECs ranging below the threshold value of 6000 mm²/mL. Based upon these in vitro findings, Pigment Blue 15:1 is classified as active.

In vivo categorization indicates Pigment Blue 15:1 passivity, thereby refuting the in vitro assignment as over-predictive For Pigment Blue 15:1, a STIS NOAEC of 30 mg/m³ was recorded [79]. At this aerosol concentration, blue pigment-laden AMs were observed in the lung parenchyma and LALNs. Further, slight epithelial hypertrophy or hyperplasia was noted in terminal bronchioles that however were assessed as rather reflecting the challenged biological clearance mechanism than adverse reactions. All findings were fully reversible within the 3-week post-exposure period. Based upon this in vivo study, Pigment Blue 15:1 is categorized as passive. Accordingly, for this pigment, the in vitro NR8383 AM assay over-predicted its toxic potential in the rat STIS.

Graphite nanoplatelets

Graphite nanoplatelets are assigned as in vitro passive Graphite nanoplatelets elicited significantly increased GLU and TNF-α levels (in vitro LOAECs, 3330 and 6660 mm²/mL, respectively. Accordingly, only one parameter (GLU) ranged below the threshold value of 6000 mm²/mL. Based upon these findings, graphite nanoplatelets are assigned as passive.

In vivo categorization confirms passivity of graphite nanoplatelets Inhalation exposure to up to 50 mg/m³ graphite nanoplatelets in a STIS did not cause any adverse effects in the rat lung as was determined by BALF evaluation, hematology and histopathological evaluation [82]. Based upon this in vivo study, graphite nanoplatelets are categorized as passive, which confirms the in vitro assignment.

Summary of in vitro–in vivo comparisons

In summary, for 19 of the 20 test materials, the in vitro NR838 AM assay addressing extracellular release of LDH, GLU, TNF-α and H_2O_2 correctly predicted in vivo activity or passivity in the rat STIS. Pigment Blue 15:1 was the only material that tested false positive: Based upon the significant in vitro LOAECs that ranged below the threshold value of 6000 mm²/mL for LDH and GLU (each: 4770 mm²/mL), 2 of the 4 in vitro parameters were positive. This resulted in Pigment Blue 15:1 assignment as active, whereas it had been categorized as passive based upon the high STIS NOAEC of 30 mg/m³.

By contrast, for SiO_2.amino, ZrO_2.TODA, DPP Orange N, and graphite nanoplatelets, only one parameter each tested positive with significant in vitro LOAECs ranging below the threshold value of 6000 mm²/mL. ZrO_2.TODA only triggered LDH, graphite nanoplatelets only triggered GLU, and SiO_2.amino and DPP Orange N each only triggered TNF-α release. By definition, this in vitro outcome resulted in their assignment as passive, and this result was confirmed by the in vivo data available for all four of these test materials.

Applying the Cooper statistics [93], the in vitro NR8383 AM assay performed under the conditions of the present study had a specificity of 91 % and a sensitivity of 100 % with an overall accuracy of 95 %. The rates for negative and positive prediction were 90 and 100 % (Table 4).

Testing against a particulate benchmark material as a NC is mandatory in an empirical assay, since it provides information on the reliability and reproducibility of the behaviour of the cells under loading conditions. When evaluating all test results against the corresponding values recorded for the negative (albeit micron-sized) benchmark material corundum (Additional file 1: Table S1), Pigment Blue 15:1 was again assessed false positive.

Wiemann *et al. J Nanobiotechnol (2016) 14:16*

Page 19 of 27

Table 4 Determination of the accuracy, sensitivity and specificity of the in vitro NR8383 alveolar macrophage assay

	Test material activity, STIS	Test material passivity, STIS	SUM	
Test material activity, in vitro	9	1	10	90 % positive prediction
Test material passivity, in vitro	0	10	10	100 % negative prediction
SUM	9	11	20	
	100 % sensitivity	91 % specificity		
	Accuracy 95 %			

Comparison of altogether 20 in vitro test results (*cf.* Table 3) to in vivo results from rat short-term inhalation studies applying the Cooper statistics [93]

Since the test results obtained for corundum were slightly higher than those recorded for the particle-free vehicle control, the corundum-based evaluation resulted in some minor deviations from the vehicle control-based evaluation. This, however, resulted in a number of statistically relevant differences. Using the corundum-based evaluation, SiO_2 NM-203 was assessed 'false negative' (only one significant LOAEC < 6000 mm^2/mL was recorded, i.e., for GLU). Furthermore, ZrO_2.TODA and SiO_2.phosphate exhibited one positive finding, each. A sharp demarcation line between active and passive materials will be prone to erroneous decisions. Therefore, the premise had been set that at least two of the four parameters had to be altered to assign a material as active. Notwithstanding, false negative findings are detrimental for regulatory toxicity testing, and for this reason the statistical evaluation against untreated cells proved superior to the evaluation against the negative benchmark material corundum. Accordingly, in the subsequent discussion, only the vehicle-control-based evaluation is addressed.

Discussion

In the present study, the in vitro NR8383 AM assay evaluating extracellular release of LDH, GLU, TNF-α and H_2O_2 under standardized conditions using protein-free culture medium proved highly accurate in distinguishing active from passive inorganic NMs or nanosized organic pigments. All nine test materials that had been categorized as active using the STIS NOAEC-based threshold value of <10 mg/m^3 laid down by Arts et al. [33] were correctly identified as active. Further, of the 11 test materials that had been categorized as passive (i.e., inert) by a STIS NOAEC of 10 mg/m^3 or higher, only one test material (Pigment Blue 15:1) was tested false positive in the in vitro NR8383 AM assay. For the other ten test materials that had been categorized as passive using the STIS NOAEC, the in vitro data correctly predicted in vivo passivity.

Test protocol, prediction model, and threshold values

All 9 NMs that were assigned as active elicited elevated levels of extracellular LDH in the in vitro NR8383 AM assay. To increase the robustness of the assay and reduce the number of false positives, it had been defined that ≥2 of the 4 in vitro parameters had to be positive in order to assign a test material as active. For 3 of the 9 active NMs, each, the increased LDH levels coincided with increased GLU levels (SiO_2 NM-200 and NM-203 and Pigment Blue 15:1), TNF-α levels (nano-CeO_2 and CeO_2 NM-211 and NM-212) or GLU plus TNF-α levels (TiO_2 NM-105, ZnO NM-111, Al-doped CeO_2). Also for the non-nanosized PC quartz DQ12, significantly elevated LDH, GLU and TNF-α were recorded, and a significant LDH level as sole affected parameter (that hence did not result in NM assignment as active) was recorded for ZrO_2.TODA.

By contrast, significant H_2O_2 formation below the in vitro threshold value of 6000 mm^2/mL was never recorded, neither as sole affected parameter, nor in combination with another affected parameter. Of note, however, a moderate to significant H_2O_2 formation was observed for the colloidal test materials (i.e., SiO_2. naked and its surface functionalized variants as well as the surface functionalized ZrO_2 NMs). The mechanism by which, e.g., SiO_2.phosphate induces H_2O_2 formation remains unknown, but it may be related to non-specific receptor activation. However, apparently, it does not depend on the presence of diffusible nanoparticles, since only three of the H_2O_2-inducing NMs (i.e., SiO_2.naked, SiO_2.amino, and SiO_2.phosphate) remained dispersed in the nanosize under the testing conditions of the present study.

It might be questioned whether the determination of ROS formation is essential for the in vitro NR8383 AM assay, especially since the STIS protocol does not foresee a directly corresponding parameter. Nevertheless, the authors of the present study suggest maintaining H_2O_2 formation as fourth parameter for the in vitro NR8383 AM assay. Different reaction patterns observed for different types of test materials may provide a first insight into their specific toxicological mechanisms which may further provide relevant information for the grouping of NMs [3, 33, 79] or the determination of adverse-outcome-pathways [115]. In this respect, also the

Wiemann *et al. J Nanobiotechnol* (2016) 14:16

Page 20 of 27

observation that only some NMs elicited significant H_2O_2 formation requires further investigations.

AMs were selected as test system for the present study because the inflammatory effects that NMs may elicit in the rat lung upon short-term inhalation are considered to emanate at least in part from stimulated or compromised AMs. Accordingly, the mechanisms leading to pulmonary inflammation and which are reflected in the corresponding NOAECs are based upon AM effects. Importantly, in developing the test protocol for the in vitro NR8383 AM assay, high accuracy of the in vitro assay was achieved by expressing data using surface area-based dose metrics (mm^2/mL) and by combining the in vitro threshold value of <6000 mm^2/mL with the 'at least 2 out of 4' prediction model to assign a test material as active. The in vitro threshold value of 6000 mm^2/mL has been set as a versatile measure to reflect the highest in vitro 'non-overload' dose under the conditions of the macrophage assay. Surface area-based dose metrics are widely accepted for the in vitro assessment of NMs since their cellular effects are conveyed by their surface [95–99, 116–120]. By contrast, prior to the present study, application of a surface area-based threshold value in an in vitro AM assay to distinguish active from passive NMs had not yet been suggested.

As outlined in "Definition of in vitro threshold value" section, the threshold of 6000 mm^2/mL was derived from 4000 μm^2/NR8383 cell. One must be aware that a sharply defined threshold value bears some uncertainty and should include some margin of safety. In this sense this threshold value has been derived from in vivo findings: Since NR8383 cells widely resemble in vivo rat AMs both in terms of morphology and biological reactivity, 4000 μm^2/NR8383 cell may be multiplied with the total number of AMs per rat lung (i.e., $1–2 \times 10^7$ [54]), resulting in a calculated particle surface area-based threshold for the rat lung of $4–8 \times 10^{10}$ μm^2 (corresponding to 0.04–0.08 m^2). Since a rat lung weighs approx. 1 g [121], the same value applies when expressing the particle surface area-based threshold per gram lung tissue (i.e., 0.04–0.08 m^2/g lung tissue). Interestingly, an earlier study addressing the sub-chronic pulmonary effects of inhaled TiO_2 and $BaSO_4$ NMs in rats suggested that the pulmonary overload of these poorly soluble particles begins at 0.02–0.03 m^2/g lung tissue [95]. Hence, the in vitro threshold values applied in the present study is approx. twofold higher as it would be if the value from Tran et al. [95] was applied. This difference may be tolerable due to some uncertainties of the above-made calculations such as dynamically changing macrophage populations. Importantly, since materials that elicit adverse effects below the calculated threshold of 0.04–0.08 m^2/g lung tissue are categorized as active in the present study, this higher threshold is conservative.

Taking into account the specific BET surface areas for different NMs, the calculated in vivo overload threshold of 0.04–0.08 m^2/lung is equivalent to, e.g., 0.2–0.4 mg SiO_2.naked (BET: 200 m^2/g); 0.6–1.2 mg CeO_2 NM-212 (BET: 66 m^2/g); or 0.85–1.7 mg TiO_2 NM-105 (BET: 47 m^2/g). Accordingly, any in vivo adverse effect observed below these lung burdens should indicate test material-specific activity in the non-overload range.

However, to convert the in vivo overload threshold of 0.04–0.08 m^2/lung to the mass-based aerosol concentration (i.e., mg/m^3), NM lung deposition needs to be taken into account. Importantly, lung burden, as measured after 5-day exposure under STIS conditions, is not only concentration-dependent, but also material-dependent [11]. Hence, also the in vivo overload threshold will be material-dependent. For instance, if a specific NM is highly soluble or has a low pulmonary deposition, its apparent lung burden may be low, and the maximum 'non-overload' aerosol concentration may be higher than for an insoluble NM that further has a high pulmonary deposition. Moreover, material properties influencing lung clearance may play a role. For instance, exposure to 0.5 mg/m^3 CeO_2 NM-212 in a rat STIS resulted in a lung burden of 0.011 mg/lung directly after 5 days of exposure and decreased to 0.006 mg/lung by the end of the 21-day post-exposure period. By contrast, exposure to 5 and 25 mg/m^3 of this same material yielded higher lung burdens with only little decrease during the post-exposure observation period, indicating impaired clearance [111]. Also the lung burdens recorded for CeO_2 NM-212 were approx. twofold higher than the ones recorded for CeO_2 NM-211 under identical conditions [111]. Accordingly, precise comparisons of in vitro and in vivo data recorded for a given test material require consideration of the measured lung burden (or of a reliable calculation thereof).

However, for practical reasons, i.e., for the prediction of NM activity or passivity under routine regulatory toxicity testing conditions, it appears advantageous to use the fixed in vitro threshold value of 6000 mm^2/mL since it is easy to apply and further includes a margin of safety. Thereby, it is conservative: In the present study, it did not generate any false negative results. By contrast, for the time being, the occurrence of few false positive results (i.e., 1 out of 11 in the present study) cannot be avoided. Nevertheless, a low false positive rate does not prevent incorporation of the in vitro NR8383 AM assay into a regulatory framework for the hazard assessment of NMs.

Finally, the in vitro threshold of 6000 mm^2/mL is compared to the threshold value of 10 $\mu g/cm^2$ cell culture surface area that Kroll et al. [17] calculated as indicating in vitro cellular overload conditions. Of note, Kroll et al. related their threshold value to the entire rat lung surface

Wiemann *et al. J Nanobiotechnol* (2016) 14:16

Page 21 of 27

area, but not to the pool of AMs. As presented above, the particle surface area-based in vitro threshold value of 6000 mm^2/mL corresponds to 3600 mm^2/cm^2 cell culture surface area (for a cell culture volume of 200 μL). BET surface areas of the test materials applied in the present study ranged from 15 m^2/g (i.e., 15 mm^2/μg) for ZnO NM-111 to 200 m^2/g (i.e., 200 mm^2/μg) for the colloidal SiO$_2$ NMs and pyrogenic SiO$_2$ NM-203. Accordingly, for ZnO NM-111, the 6000 mm^2/mL threshold value equals 240 μg/cm^2; for test materials with a BET surface area of approx. 60 m^2/g (CeO$_2$ NM-211 or DPP Orange N) it equals 60 μg/cm^2, and for the mentioned SiO$_2$ NMs it equals 18 μg/cm^2. Therefore, the in vitro threshold set in the present study is higher than the in vitro threshold set by Kroll et al. [17]. However, this is not surprising since the threshold set in the present study considers the pool of AMs as a cell compartment that actively collects particles, both in vitro and in vivo.

Applicability domain of the in vitro NR8383 AM assay
All test materials that were identified as active in vitro or in vivo elicited inflammatory effects in the rat lung. In the STIS, this was indicated by elevated PMN counts in the BALF that frequently coincided with increased total protein values and enzyme activities. These early pro-inflammatory reactions became evident and were easily quantifiable by BALF analysis, whereas histopathological evaluation mostly revealed moderate alterations of the lung tissue that were possibly secondary to the inflammation. Accordingly, the in vitro determination of a NM's activity allows predicting its inflammatory potential in the rat lung. This may include cytotoxic or AM-activating effects upon inhalation and deposition in the rat lung, and/or the evolvement of inflammatory responses secondary to its AM-activating effects.

Although the response of a NR8383 cell to a NM may, to a certain degree, be taken as being representative for other cells as well [68, 69], AM-independent, direct effects of NMs on epithelial cells or other pulmonary cells, which may also contribute to the overall pulmonary response to NMs (e.g., the epithelial cytokine response) are not covered by the in vitro NR8383 AM assay. Other in vitro test systems than AMs may reflect epithelial disorders evolving in the lung [122]. Nevertheless, also AMs may be suitable to assess such effects since they are either directly or indirectly involved in many pulmonary disorders. For instance, an impaired lung clearance resulting from compromised AM activity may lead to progressive pulmonary inflammation followed by e.g., fibrosis or neoplastic transformation. This is highlighted by the examples of quartz DQ12 or CeO$_2$ NMs. These materials were assigned as active in the in vitro NR8383 AM assay. Upon chronic inhalation exposure, both materials may

elicit fibrotic alterations of the lung. Of note, however, no neoplastic changes were reported upon treatment with CeO$_2$ NMs [105, 109, 123].

As the spectrum of test materials selected for the present study and further in-house experience reveal, the in vitro NR8383 AM assay is applicable to poorly soluble low-toxicity particles (PSLT [124]) that are also called respirable granular biodurable particles (GBP [32]). Similarly, nuisance or inert dusts may be assessed, as long as they may be dispersed in the culture medium. Also particles retrieved from air filters, such as welding fumes or particles released from dental materials upon grinding, have been tested using the standard concentration range of 22.5–180 μg/mL. Particle agglomeration and gravitational settling were found to enhance the delivery of the applied dose to the AMs at the bottom of the culture vessels. In vitro particokinetics (i.e., particle size distribution and particle agglomeration) were controlled with phase contrast microscopy combined with tracking analysis of the supernatant. In fact, only 7 of the 20 test materials (SiO$_2$.naked, SiO$_2$.amino, SiO$_2$.phosphate, SiO$_2$ NM-203, Fe$_2$O$_3$, and the two organic pigments) remained at least partially dispersed in the culture media. As a result, the effective cellular dose of these materials cannot be determined with certainty using the simple microscopic characterization methods applied in the present study.

Nevertheless, there are indeed NMs which cannot be successfully tested in the in vitro NR8383 AM assay for technical reasons. For instance, while MWCNT NM-401 could be assessed (data not shown), other MWCNTs could not be dispersed sufficiently well to allow testing. Materials, which form agglomerates that float in suspension or which escape uptake by the AMs by adhering to the vessel walls or by gathering at the surface due to low buoyant density, can also not be assessed. Furthermore, materials which strongly interfere with the optical read out may cause problems, since the transmitted light levels may by too low to be corrected by the cell-free controls. Of note, however, the orange, red, and blue pigments could be evaluated since the AMs took them up and completely cleared the cell culture bottom from coloured agglomerates.

Test material effects
In the following, the specific in vitro effects of the test materials observed in the in vitro NR8383 AM assay are compared to the findings reported for identical or comparable test materials available in the published literature.

Active metal oxide NMs (TiO$_2$, ZnO, CeO$_2$)
Generally, the in vitro findings recorded for the six metal oxide NMs that were identified as active (TiO$_2$ NM-105, ZnO NM-111, and all four tested CeO$_2$ NMs) stand in

Wiemann *et al. J Nanobiotechnol* (2016) 14:16

Page 22 of 27

line with results from other in vitro or in vivo studies. Recently, anatase TiO_2 NM-101 has been found to elicit weak activating effects on HL-60 cells which may represent human neutrophil-like cells [125]. In the same study, the ion-shedding ZnO NM-110 and Ag NM-300 elicited much more pronounced cytotoxicity. Consistent with these findings, also uncoated and coated ZnO NMs (*cf.* "Active metal oxide NMs (TiO2, ZnO, CeO2)" section) as well as Ag NM-300K (data not shown) were recorded as active in the in vitro NR8383 AM assay. Even though rat STIS data are unavailable for Ag NM-300K, these findings appear biologically relevant.

CeO_2 NMs have a highly reactive surface which, apart from Ce^{4+} and Ce^{3+}, is chiefly composed of oxygen and O^{2-}. The change of oxidation state from $3+$ to $4+$ appears to determine the biological activity of CeO_2 NMs. This may either result in ROS generating or ROS scavenging properties [21, 88]. Accordingly, different types of CeO_2 NMs may be expected to elicit contradictory reactions, and different CeO_2 NMs have indeed been observed to be either ROS/H_2O_2 protective [126, 127] or toxic in rats [123] or in different types of cultured cells [68].

However, the four different CeO_2 NMs were consistently assigned as active both in vitro and in vivo. Nevertheless, based upon an in-depth evaluation of the data (*cf.* Additional file 1: Table S2), Al-doped CeO_2 NMs elicited the most pronounced inflammatory reactions observed for CeO_2 NMs in the present in vitro study (or in the published in vivo STIS data reflecting AM-based reactions in the rat lung). Especially Al-doping of CeO_2 NMs has been recognized to strongly increase the O_2-binding capacity of this material [128]. It may be assumed that O_2-surface binding may be involved in its in vitro or in vivo toxicity. Further in vitro investigations should aim at addressing the specific mechanisms of toxicity or protective cellular effects that different types of CeO_2 may elicit.

Amorphous SiO_2 NMs
Of the four different colloidal SiO_2 NMs submitted to the present study, only the unmodified SiO_2.naked was tested positive in the rat STIS [11]. An instillation study with mice provided the same outcome for these same materials [129]. Furthermore, it revealed a weak effect on PMN recruitment into the lungs for SiO_2.amino and SiO_2. phosphate. In the present study, SiO_2.amino elicited significant TNF-α release (only this one parameter affected), whereas for SiO_2.phosphate none of the four parameters were affected. The effects of SiO_2.naked recorded in the present study occurred in the absence of protein, since protein coating with fetal calf serum mitigates the toxicity of SiO_2 NMs [21, 130]. It may be assumed that the protein-binding capacity of amorphous SiO_2 may affect specific inflammatory or toxic responses in vivo.

Concordantly, surface functionalization with PEG, amino or phosphate residue may reduce or affect protein binding, both in vitro and in vivo.

Passive metal oxide and metal sulphate NMs (AlOOH, BaSO$_4$, Fe$_2$O$_3$, ZrO$_2$)
Based upon the in vitro NR8383 AM data, AlOOH and $BaSO_4$ NM-220 were assigned as passive. This result stands in full concordance with previous studies using a broad spectrum of different cell lines, including RAW264.7 macrophages, even though these studies were conducted in the presence of serum [17]. Also nanosized Fe_2O_3 (hematite) was assigned as passive. Its effects on LDH or GLU release were in the same range as its non-nanosized counterpart (data not shown). Hence, 'nanosize' of this inorganic pigment does not appear to augment its hazard potential.

In the present study, ZrO_2.TODA, but not ZrO_2. acrylate, elicited an increased LDH level (and a significant in vitro LOAEC was recorded for only this one parameter). ZrO_2.TODA and ZrO_2.acrylate also gradually differed with respect to the induced (albeit not significant) release of GLU and H_2O_2. This may point to differences caused by the different surface functionalizations. These minor findings do not correspond to the outcomes of the available STISs where neither material caused any effects up to 50 mg/m^3 [11]. Nevertheless, different STIS lung burdens were measured for ZrO_2.TODA (693 μg) and ZrO_2.acrylate (169 μg) after 5-day inhalation exposure to identical aerosol concentrations of 50 mg/m^3 [11], such that a final comparison cannot be made.

Nanosized organic pigments and graphite nanoplatelets
Coloured and dense materials are potentially difficult to evaluate in in vitro assays using colorimetric assays. Nevertheless, in the present study the two nanosized organic pigments (just as the inorganic red pigment Fe_2O_3) had mostly settled by the end of the incubation period, and further particles could be removed from the supernatant by centrifugation before the optical measurements. Thereby, an acceptable degree of variation was ensured. Also the influence of the few remaining particles could be circumvented by subtracting the values obtained for the cell-fee controls. Whereas the particles that remained in suspension (and hence did not sediment towards the cells) are not expected to affect the effective dose reaching the cells within the incubation period to a considerable extent, the precise effective cellular dose of these materials cannot be estimated.

For DPP Orange N only a dose-dependent formation of TNF-α was recorded, and just as its non-nanosized counterpart DPP Orange B, it was assigned as in vitro passive. Hence, also for this organic pigment there is

Wiemann *et al. J Nanobiotechnol (2016) 14:16*

Page 23 of 27

no indication that the 'nanosize' increases its hazard potential.

Pigment Blue 15:1 significantly increased both LDH and GLU and the calculated values were below the threshold of 6000 mm^2/mL. Thereby, this organic pigment delivered the only false positive result since it did not elicit adverse effects in vivo in the rat STIS up to aerosol concentrations of 30 mg/m^3 [79]. Even though Pigment Blue 15:1 contains copper, this compound is tightly bound to the molecule, and ions are neither released in water, nor in biological media [79]. It must be underlined that the effects that Pigment Blue 15:1 elicited in vitro were not severe: Even a mean cellular load of 30 pg/AM (equivalent to 45 μg/mL) did not lead to cell membrane damage (*cf.* Table 2). However, at this concentration, the GLU release from the intact cells was already increased, and both parameters were significantly affected at 90 and 180 μg/mL. Even though no release of copper was measured, it is known that copper ions may affect GLU expression in cells [131–133]. Obviously, the disparity between the in vitro and STIS findings recorded for Pigment Blue 15:1 remains to be investigated in further detail.

Conclusion

Investigating a broad spectrum of 18 inorganic NMs and 2 nanosized organic pigments, the in vitro NR8383 AM assay allowed distinguishing active from passive nanomaterials. AMs were selected as test system due to the predominant role these cells play in clearing the lung from inhaled particles. Further, many secondary pulmonary effects are also initiated or accompanied by AMs. The selected parameters, LDH, GLU, TNF-α and H$_2$O$_2$ formation and release, in combination with the 'at least 2 out of 4' prediction model proved easy to use and suitable for routine testing. Importantly, the model was highly efficient in predicting in vivo STIS hazard potential. Recently, application of the in vitro NR8383 AM assay within the DF4nanoGrouping Decision-making framework for the grouping and testing of NMs has shown that this assay also allows grouping NMs by biological activity [33, 79]. When integrated into a tiered testing approach, such as the DF4nanoGrouping, the in vitro NR8383 AM assay may substantially reduce the need for animal testing addressing the inhalation route of exposure. Further work should aim at validating this assay.

Additional file

> **Additional file 1: Table S1.** Comparison of significant in vitro LOAECs (significant as compared to the negative benchmark material corundum) to NOAECs and LOAECs recorded in rat STISs. **Table S2.** Bioactivity of four types of CeO$_2$ NMs in rat STISs as compared to cellular effects recorded in the in vitro NR8383 AM assay.

Abbreviations

AM: alveolar macrophage; AP: alkaline phosphatase; BALF: bronchoalveolar lavage fluid; BET: (method of) Brunauer, Teller, and Emmett; CINC: cytokine-induced neutrophil chemoattractant; DPP: diketopyrrolopyrrol; ECETOC: European Centre for the Ecotoxicology and Toxicology of Chemicals; ECHA: European Chemicals Agency; FCS: fetal calf serum; GBP: respirable granular biodurable (particles); GGT: γ-Glutamyltransferase; GLU: β-Glucuronidase; IL: interleukin; JRC: Joint Research Centre (of the EU Commission); KRPG: Krebs–Ringer phosphate glucose; LALN: lung-associated lymph node; LDH: lactate dehydrogenase; LOAEC: lowest-observed effect concentration; LPS: lipopolysaccharide; MCP: monocyte chemoattractant protein; MWCNT: multi-walled carbon nanotube; NAG: N-acetyl-glucosaminidase; NAPDH: nicotinamide adenine dinucleotide phosphate-oxidase; NC: negative control; NIOSH: National Institute for Occupational Safety and Health; NM: nanomaterial; OD: optical density; OECD: Organisation for Economic Co-operation and Development; OEL: occupational exposure limit; PBS: phosphate buffered saline; PC: positive control; PDGF: platelet-derived growth factor; PMN: polymorphonuclear neutrophil; PPS: primary particle size; PSLT: poorly soluble–low toxicity; REACH: registration, evaluation, authorisation and restriction of chemicals; ROS: reactive oxygen species; SD: standard deviation; STIS: short-term rat inhalation study; TG: test guideline; TGF-β: transforming growth factor β; TNF-α: tumour necrosis factor α; WPMN: working party on manufactured nanomaterials.

Author details

^{1} IBR R&D gGmbH Institute for Lung Health, Mendelstraße 11, 48149 Münster, Germany. ^{2} Scientific Consultancy - Animal Welfare, Hallstattfeld 16, 85579 Neubiberg, Germany. ^{3} BASF SE, Experimental Toxicology and Ecology, GB/TB - Z470, 67056 Ludwigshafen, Germany.

References

1. Regulation (EC) No 1907/2006 of the European Parliament and of the Council of 18 December 2006 concerning the Registration, Evaluation, Authorisation and Restriction of Chemicals (REACH), establishing a European Chemicals Agency, amending Directive 1999/45/EC and repealing Council Regulation (EEC) No 793/93 and Commission Regulation (EC) No 1488/94 as well as Council Directive 76/769/EEC and Commission Directives 91/155/EEC, 93/67/EEC, 93/105/EC and 2000/21/EC. OJ L. 2006;396:1.
2. EU Commission recommendation on the definition of nanomaterial. OJ L 2011;275:38.
3. Arts JH, Hadi M, Keene AM, Kreiling R, Lyon D, Maier M, Michel K, Petry T, Sauer UG, Warheit D, Wiench K, Landsiedel R. A critical appraisal of

Wiemann *et al. J Nanobiotechnol (2016) 14:16*

Page 24 of 27

existing concepts for the grouping of nanomaterials. Regul Toxicol Pharmacol. 2014;70:492–506.

4. Directive 2010/63/EU of the European Parliament and of the Council of 22 September 2010 on the protection of animals used for scientific purposes. OJ L. 2010;276:33.

5. Russell WMS, Burch RL. The principles of humane experimental technique. London, UK. Methuen, 1959. Reprinted by UFAW, 1992: 8 Hamilton Close, South Mimms, Potters Bar, Herts EN6 3QD, England. p. 238.

6. Organisation for Economic Co-operation and Development (OECD). List of manufactured nanomaterials and list of endpoints for phase one of the OECD testing programme. Series on the safety of manufactured nanomaterials. No. 6, ENV/JM/MONO(2008)13/REV, 2008.

7. Organisation for Economic Co-operation and Development (OECD). Guidance manual for the testing of manufactured nanomaterials: OECD's sponsorship programme, ENV-JM-MONO(2009)20-REV, 2010.

8. Aitken RA, Bassan A, Friedrichs S, Hankin SM, Hansen SF, Holmqvist J, Peters SAK, Poland CA, Tran CL. Specific advice on exposure assessment and hazard/risk characterisation for nanomaterials under REACH (RIP-oN 3). Final project report. REACH-NANO consultation, RNC/RIP-oN3/FPR/1/FINAL, 2011.

9. Klein CL, Wiench K, Wiemann M, Ma-Hock L, van Ravenzwaay B, Landsiedel R. Hazard identification of inhaled nanomaterials: making use of short-term inhalation studies. Arch Toxicol. 2012;86:1137–51.

10. Ma-Hock L, Burkhard S, Strauss V, Gamer AO, Wiench K, van Ravenzwaay B, Landsiedel R. Development of a short-term inhalation test in the rat using nano-titanium dioxide as a model substance. Inhal Toxicol. 2009;21:102–18.

11. Landsiedel R, Ma-Hock L, Hofmann T, Wiemann M, Strauss V, Treumann S, Wohlleben W, Groeters S, Wiench K, van Ravenzwaay B. Application of short-term inhalation studies to assess the inhalation toxicity of nanomaterials. Part Fibre Toxicol. 2014;11:16.

12. Organisation for Economic Co-operation and Development (OECD) guidelines for the testing of chemicals, Section 4. Test No. 412: Subacute inhalation toxicity: 28-day study. Adopted 8 Sep 2009.

13. Rothen-Rutishauser BM, Kiama SG, Gehr P. A three-dimensional cellular model of the human respiratory tract to study the interaction with particles. Am J Respir Cell Mol Biol. 2005;32:281–9.

14. Stone V, Johnston H, Schins RPF. Development of in vitro systems for nanotoxicology: methodological considerations. Crit Rev Toxicol. 2009;39:613–26.

15. Hackenberg S, Scherzed A, Technau A, Kessler M, Froelich K, Ginzkey C, Koehler C, Burghartz M, Hagen R, Kleinsasser N. Cytotoxic, genotoxic and proinflammatory effects of zinc oxide nanoparticles in human nasal mucosa cells in vitro. Toxicol In Vitro. 2011;25:657–63.

16. Hirsch C, Roesslein M, Krug HF, Wick P. Nanomaterial cell interactions: are current in vitro tests reliable? Nanomed. 2011;6:837–47.

17. Kroll A, Dierker C, Rommel C, Hahn D, Wohlleben W, Schulze-Isfort C, Göbbert C, Voetz M, Hardinghaus F, Schnekenburger J. Cytotoxicity screening of 23 engineered nanomaterials using a test matrix of ten cell lines and three different assays. Part Fibre Toxicol. 2011;8:9.

18. Gasser M, Wick P, Clift MJ, Blank F, Diener L, Yan B, Gehr P, Krug HF, Rothen-Rutishauser B. Pulmonary surfactant coating of multi-walled carbon nanotubes (MWCNTs) influences their oxidative and pro-inflammatory potential *in vitro*. Part Fibre Toxicol. 2012;9:17.

19. Nel AE, Xia T, Meng H, Wang X, Lin S, Ji Z, Zhang H. Nanomaterial toxicity testing in the 21st century: use of a predictive toxicological approach and highthroughput screening. Acc Chem Res. 2013;46:607–21.

20. Nel AE, Nasser E, Godwin H, Avery D, Bahadori T, Bergeson L, Beryt E, Bonner JC, Boverhof D, Carter J, Castranova V, Deshazo JR, Hussain SM, Kane AB, Klaessig F, Kuempel E, Lafranconi M, Landsiedel R, Malloy T, Miller MB, Morris J, Moss K, Oberdörster G, Pinkerton K, Pleus RC, Shatkin JA, Thomas R, Tolaymat T, Wang A, Wong J. A multi-stakeholder perspective on the use of alternative test strategies for nanomaterial safety assessment. ACS Nano. 2013;7:6422–33.

21. Landsiedel R, Sauer UG, Ma-Hock L, Schnekenburger J, Wiemann M. Pulmonary toxicity of nanomaterials: a critical comparison of published in vitro assays with in vivo inhalation or instillation studies. Nanomed. 2014;9:2557–85.

22. International Commission on Radiological Protection. (ICRP) publication No. 66. Human respiratory tract model for radiological protection. Ann ICRP. 1994;24:1–3.

23. Morrow PE. Possible mechanisms to explain dust overloading of the lungs. Fund Appl Toxicol. 1988;10:369–84.

24. Morrow PE. Dust overloading of the lungs: update and appraisal. Toxicol Appl Pharmacol. 1992;113:1–12.

25. Bakand S, Winder C, Khalil C, Hayes A. Toxicity assessment of industrial chemicals and airborne contaminants: transition from in vivo to in vitro test methods: a review. Inhal Toxicol. 2005;17:775–87.

26. Oberdörster G, Oberdörster E, Oberdörster J. Nanotoxicology: an emerging discipline evolving from studies of ultrafine particles. Environ Health Perspect. 2005;113:823–39.

27. Anttila S. Dissolution of stainless steel welding fumes in the rat lung: an x ray microanalytical study. Br J Ind Med. 1986;43:592–6.

28. Gosens I, Post JA, de la Fonteyne LJ, Jansen EH, Geus JW, Cassee FR, de Jong WH. Impact of agglomeration state of nano- and submicron sized gold particles on pulmonary inflammation. Part Fibre Toxicol. 2010;7:37.

29. Morfeld P, Treumann S, Ma-Hock L, Bruch J, Landsiedel R. Deposition behaviour of inhaled nanostructured TiO_2 in rats: fractions of particle diameter below 100 nm (nanoscale) and the slicing bias of transmission electron microscopy. Inhal Toxicol. 2012;24:939–51.

30. Kreyling WG, Semmler-Behnke M, Seitz J, Scymczak W, Wenk A, Mayer P, Takenaka S, Oberdörster G. Size dependence of the translocation of inhaled iridium and carbon nanoparticle aggregates from the lung of rats to the blood and secondary target organs. Inhal Toxicol. 2009;21(Suppl 1):55–60.

31. Kreyling WG, Semmler-Behnke M, Takenaka S, Möller W. Differences in the biokinetics of inhaled nano- versus micrometer-sized particles. Acc Chem Res. 2013;46:714–22.

32. Moreno-Horn M, Gebel T. Granular biodurable nanomaterials: no convincing evidence for systemic toxicity. Crit Rev Toxicol. 2014;44:849–75.

33. Arts JH, Hadi M, Irfan MA, Keene AM, Kreiling R, Lyon D, Maier M, Michel K, Petry T, Sauer UG, Warheit D, Wiench K, Wohlleben W, Landsiedel R. A decision-making framework for the grouping and testing of nanomaterials (DF4nanoGrouping). Regul Toxicol Pharmacol. 2015;71(Suppl 2):S1–27.

34. Oberdörster G, Ferin J, Lehnert BE. Correlation between particle size, in vivo particle persistence, and lung injury. Environ Health Perspect. 1994;102(Suppl 5):173–9.

35. Semmler-Behnke M, Takenaka S, Fertsch S, Wenk A, Seitz J, Mayer P, Oberdörster G, Kreyling WG. Efficient elimination of inhaled nanoparticles from the alveolar region: evidence for interstitial uptake and subsequent reentrainment onto airways epithelium. Environ Health Perspect. 2007;115:728–33.

36. ECETOC. European Centre for the Toxicology and Ecotoxicology of Chemicals Technical Report TR 122. Poorly soluble particles. Lung overload. ISSN-0773-8072-122, 2013.

37. Pauluhn J. Derivation of occupational exposure levels (OELs) of low-toxicity isometric biopersistent particles: how can the kinetic lung overload paradigm be used for improved inhalation toxicity study design and OEL-derivation? Part Fibre Toxicol. 2014;11:72.

38. Rimal B, Greenberg AK, Rom WN. Basic pathogenetic mechanisms in silicosis: current understanding. Curr Opin Pulm Med. 2005;11:169–73.

39. Sun B, Wang X, Ji Z, Wang M, Liao YP, Chang CH, Li R, Zhang H, Nel AE, Xia T. NADPH oxidase-dependent NLRP3 inflammasome activation and its important role in lung fibrosis by multiwalled carbon nanotubes. Small. 2015;11:2087–97.

40. Farcal LR, Uboldi C, Mehn D, Giudetti G, Nativo P, Ponti J, Gilliland D, Rossi F, Bal-Price A. Mechanisms of toxicity induced by SiO_2 nanoparticles of in vitro human alveolar barrier: effects on cytokine production, oxidative stress induction, surfactant proteins A mRNA expression and nanoparticles uptake. Nanotoxicol. 2013;7:1095–110.

41. Herold S, Mayer K, Lohmeyer J. Acute lung injury: how macrophages orchestrate resolution of inflammation and tissue repair. Front Immunol. 2011;2:65.

42. Becker S, Devlin RB, Haskill JS. Differential production of tumor necrosis factor, macrophage colony stimulating factor, and interleukin 1 by human alveolar macrophages. J Leukoc Biol. 1989;45:353–61.

43. Driscoll KE, Lindenschmidt RC, Maurer JK, Higgins JM, Ridder G. Pulmonary response to silica or titanium dioxide: inflammatory cells, alveolar

Wiemann *et al. J Nanobiotechnol (2016) 14:16*

Page 25 of 27

macrophage-derived cytokines, and histopathology. Am J Respir Cell Mol Biol. 1990;2:381–90.

44. Driscoll KE, Higgins JM, Leytart MJ, Crosby LL. Differential effects of mineral dusts on the in vitro activation of alveolar macrophage eicosanoid and cytokine release. Toxicol In Vitro. 1990;4:284–8.

45. Driscoll KE, Carter JM, Howard BW, Hassenbein DG, Pepelko W, Baggs RB, Oberdörster G. Pulmonary inflammatory, chemokine, and mutagenic responses in rats after subchronic inhalation of Carbon Black. Toxicol Appl Pharmacol. 1995;136:372–80.

46. Von Essen SG, Robbins RA, Thompson AB, Ertl RF, Linder J, Rennard S. Mechanisms of neutrophil recruitment to the lung by grain dust exposure. Am Rev Respir Dis 1988, 138:921-927. Erratum in: Am Rev Respir Dis. 1989;139:1065.

47. Schnyder J, Baggiolini M. Secretion of lysosomal hydrolases by stimulated and nonstimulated macrophages. J Exp Med. 1978;48:435–50.

48. Joseph M, Tonnel AB, Torpier G, Capron A, Arnoux B, Benveniste J. Involvement of immunoglobulin E in the secretory processes of alveolar macrophages from asthmatic patients. J Clin Invest. 1983;71:221–30.

49. Giannattasio G, Lai Y, Granata F, Mounier CM, Nallan L, Oslund R, Leslie CC, Marone G, Lambeau G, Gelb MH, Triggiani M. Expression of phospholipases A2 in primary human lung macrophages: role of cytosolic phospholipase A2-alpha in arachidonic acid release and platelet activating factor synthesis. Biochim Biophys Acta. 2009;1791:92–102.

50. Bruch J, Rehn S, Rehn B, Borm PJ, Fubini B. Variation of biological responses to different respirable quartz flours determined by a vector model. Int J Hyg Environ Health. 2004;207:203–16.

51. Barlow PG, Brown DM, Donaldson K, MacCallum J, Stone V. Reduced alveolar macrophage migration induced by acute ambient particle (PM10) exposure. Cell Biol Toxicol. 2008;24:243–52.

52. Liu R, Zhang X, Pu Y, Yin L, Li Y, Zhang X, Liang G, Li X, Zhang J. Small-sized titanium dioxide nanoparticles mediate immune toxicity in rat pulmonary alveolar macrophages in vivo. J Nanosci Nanotechnol. 2010;10:5161–9.

53. Morales-Nebreda L, Misharin AV, Perlman H, Budinger GR. The heterogeneity of lung macrophages in the susceptibility to disease. Eur Respir Rev. 2015;24:505–9.

54. Rehn B, Bruch J, Zou T, Hobusch G. Recovery of rat alveolar macrophages by bronchoalveolar lavage under normal and activated conditions. Environ Health Perspect. 1992;97:11–6.

55. Rehn B, Rehn S, Bruch J. Ein neues in vitro-Prüfkonzept (Vektorenmodell) zum biologischen Screening und Monitoring der Lungentoxizität von Stäuben. Gefahrstoffe—Reinhaltung der Luft. 1999;59:181–188.

56. Morgan A, Moores SR, Holmes A, Evans JC, Evans NH, Black A. The effect of quartz, administered by instillation, on the lung I. The cellular response. Environ Res. 1980;22:1–12.

57. Bruch J, Rehn B, Duval-Arnould G, Efskind J, Röderer G, Sébastian P. Toxicological investigations on the respirable fraction of silicon carbide grain products by the in vitro vector model. Inhal Toxicol. 2014;26:278–88.

58. Pauluhn J. Pulmonary toxicity and fate of agglomerated 10 and 40 nm aluminum oxyhydroxides following 4-week inhalation exposure of rats: toxic effects are determined by agglomerated, not primary particle size. Toxicol Sci. 2009;109:152–67.

59. Chen W, Stempelmann K, Rehn S, Diederichs H, Rehn B, Bruch J. Biological responses of workplace particles and their association with adverse health effects on miners. J Environ Monit. 2004;6:967–72.

60. Helmke RJ, Boyd RL, German VF, Mangos JA. From growth factor dependence to growth factor responsiveness: the genesis of an alveolar macrophage cell line. In Vitro Cell Dev Biol. 1987;23:567–74.

61. Helmke RJ, German VF, Mangos JA. A continuous alveolar macrophage cell line: comparisons with freshly derived alveolar macrophages. In Vitro Cell Dev Biol. 1989;25:44–8.

62. Koslowski R, Seidel D, Kuhlisch E, Knoch KP. Evidence for the involvement of TGF-beta and PDGF in the regulation of prolyl 4-hydroxylase and lysyloxidase in cultured rat lung fibroblasts. Exp Toxicol Pathol. 2003;55:257–64.

63. Albrecht C, Höhr D, Haberzettl P, Becker A, Borm PJ, Schins RP. Surface-dependent quartz uptake by macrophages: potential role in pulmonary inflammation and lung clearance. Inhal Toxicol. 2007;19(Suppl 1):39–48.

64. Scherbart AM, Langer J, Bushmelev A, van Berlo D, Haberzettl P, van Schooten FJ, Schmidt AM, Rose CR, Schins RP, Albrecht C. Contrasting

65. macrophage activation by fine and ultrafine titanium dioxide particles is associated with different uptake mechanisms. Part Fibre Toxicol. 2011;8:31.

66. Bhattacharjee S, Ershov D, Fytianos K, van der Gucht J, Alink GM, Rietjens IM, Marcelis AT, Zuilhof H. Cytotoxicity and cellular uptake of tri-block copolymer nanoparticles with different size and surface characteristics. Part Fibre Toxicol. 2012;9:11.

66. Bhattacharjee S, de Haan LH, Evers NM, Jiang X, Marcelis AT, Zuilhof H, Rietjens IM, Alink GM. Role of surface charge and oxidative stress in cytotoxicity of organic monolayer-coated silicon nanoparticles towards macrophage NR8383 cells. Part Fibre Toxicol. 2010;7:25.

67. Ronzani C, Safar R, Diab R, Chevrier J, Paoli J, Abdel-Wahhab MA, Le Faou A, Rihn BH, Joubert O. Viability and gene expression responses to polymeric nanoparticles in human and rat cells. Cell Biol Toxicol. 2014;30:137–46.

68. Cho WS, Duffin R, Bradley M, Megson IL, Macnee W, Lee JK, Jeong J, Donaldson K. Predictive value of in vitro assays depends on the mechanism of toxicity of metal oxide nanoparticles. Part Fibre Toxicol. 2013;10:55.

69. Lison D, Laloy J, Corazzari I, Muller J, Rabolli V, Panin N, Huaux F, Fenoglio I, Fubini B. Sintered indium-tin-oxide (ITO) particles: a new pneumotoxic entity. Toxicol Sci. 2009;108:472–81.

70. Lison D, Thomassen LC, Rabolli V, Gonzalez L, Napierska D, Seo JW, Kirsch-Volders M, Hoet P, Kirschhock CE, Martens JA. Nominal and effective dosimetry of silica nanoparticles in cytotoxicity assays. Toxicol Sci. 2008;104:155–62.

71. Pulskamp K, Diabaté S, Krug HF. Carbon nanotubes show no sign of acute toxicity but induce intracellular reactive oxygen species in dependence on contaminants. Toxicol Lett. 2007;168:58–74.

72. Wagner AJ, Bleckmann CA, Murdock RC, Schrand AM, Schlager JJ, Hussain SM. Cellular interaction of different forms of aluminum nanoparticles in rat alveolar macrophages. J Phys Chem B. 2007;111:7353–9.

73. Eidi H, Joubert O, Attik G, Duval RE, Bottin MC, Hamouia A, Maincent P, Rihn BH. Cytotoxicity assessment of heparin nanoparticles in NR8383 macrophages. Int J Pharm. 2010;396:156–65.

74. Eidi H, Joubert O, Némos C, Grandemange S, Mograbi B, Foliguet B, Tournebize J, Maincent P, Le Faou A, Aboukhamis I, Rihn BH. Drug delivery by polymeric nanoparticles induces autophagy in macrophages. Int J Pharm. 2012;422:495–503.

75. Bhattacharjee S, Rietjens IM, Singh MP, Atkins TM, Purkait TK, Xu Z, Regli S, Shukaliak A, Clark RJ, Mitchell BS, Alink GM, Marcelis AT, Fink MJ, Veinot JG, Kauzlarich SM, Zuilhof H. Cytotoxicity of surface-functionalized silicon and germanium nanoparticles: the dominant role of surface charges. Nanoscale. 2013;5:4870–83.

76. Kuempel ED, Castranova V, Geraci CL, Schulte PA. Development of risk-based nanomaterial groups for occupational exposure control. J Nanopart Res. 2012;14:1029–43.

77. Bruch J, Rehn B, Song H, Gono E, Malkusch W. Toxicological investigations on silicon carbide. 1. Inhalation studies. Br J Ind Med. 1993;50:797–806.

78. Bruch J, Rehn B, Song H, Gono E, Malkusch W. Toxicological investigations on silicon carbide. 2. In vitro cell tests and long term injection tests. Br J Ind Med. 1993;50:807–13.

79. Arts JH, Irfan MA, Keene AM, Kreiling R, Lyon D, Maier M, Michel K, Neubauer N, Petry T, Sauer UG, Warheit D, Wiench K, Wohlleben W, Landsiedel R. Case studies putting the decision-making framework for the grouping and testing of nanomaterials (DF4nanoGrouping) into practice. Regul Toxicol Pharmacol. 2015. doi:10.1016/j.yrtph.2015.11.020.

80. Arts JH, Muijser H, Duistermaat E, Junker K, Kuper CF. Five-day inhalation toxicity study of three types of synthetic amorphous silicas in Wistar rats and post-exposure evaluations for up to 3 months. Food Chem Toxicol. 2007;45:1856–67.

81. Van Ravenzwaay B, Landsiedel R, Fabian E, Burkhardt S, Strauss V, Ma-Hock L. Comparing fate and effects of three particles of different surface properties: nano-TiO_2, pigmentary TiO_2 and quartz. Toxicol Lett. 2009;186:152–9.

82. Ma-Hock L, Strauss V, Treumann S, Küttler K, Wohlleben W, Hofmann T, Gröters S, Wiench K, van Ravenzwaay B, Landsiedel R. Comparative inhalation toxicity of multi-wall carbon nanotubes, graphene, graphite nanoplatelets and low surface carbon black. Part Fibre Toxicol. 2013;10:23.

Wiemann *et al. J Nanobiotechnol (2016) 14:16*

Page 26 of 27

83. Driessen MD, Mues S, Vennemann A, Hellack B, Bannuscher A, Vimalakanthan V, Riebeling C, Ossig R, Wiemann M, Schnekenburger J, Kuhlbusch TA, Renard B, Luch A, Haase A. Proteomic analysis of protein carbonylation: a useful tool to unravel nanoparticle toxicity mechanisms. Part Fibre Toxicol. 2015;12:36.

84. Kuhlbusch TAJ, Krug HF, Nau K, editors. NanoCare—Health related effects of nanoparticles. Frankfurt: Final scientific report Dechema eV; 2009.

85. Hellack B, Hülser T, Izak E, Kuhlbusch T, Meyer F, Spree M, Voetz M, Wiggers H, Wohlleben W. Characterization of all nanoGEM materials. 2013, accessible at: www.nanogem.de.

86. Izak-Nau E, Voetz M. As-produced: Intrinsic physico-chemical properties and appropriate characterization tools. In: Wohlleben W, Kuhlbusch T, Schnekenburger J, Lehr C-M, editors. Nanomaterials Throughout their Lifecycles: Safety. Boca Raton: Human Hazard and Exposure. Taylor & Francis; 2014.

87. Singh C, Friedrichs S, Levin M, Birkedal R, Jensen KA, Pojana G, Wohlleben W, Schulte S, Wiench K, Turney T, Koulaeva O, Marshall D, Hund-Rinke K, Koerdel W, van Doren E, De Temmerman PJ, Abi Daoud FM, Mast J, Gibson N, Koeber R, Linsinger T, Klein CL. NM series of representative manufactured nanomaterials, zinc oxide NM-110, NM-111, NM-112, NM-113. Characterisation and test item preparation. EUR 25066 EN, 2011.

88. Singh C, Friedrichs S, Ceccone G, Gibson P, Jensen KA, Levin M, Goenaga Infante H, Carlander D, Rasmussen K. Cerium dioxide, NM-211, NM-212, NM-213. Characterisation and test item preparation. EUR 26649 EN, 2014.

89. Rasmussen K, Mech A, Mast J, De Temmerman PJ, Waegeneers N, Van Steen F, Pizzolon JC, De Temmerman L, van Doren E, Alstrup Jensen K, Birkedal R, Levin M, Hjortkjær Nielsen S, Kalevi Koponen I, Clausen PA, Kembouche Y, Thieriet N, Spalla O, Giuot C, Rousset D, Witschger O, Bau S, Bianchi B, Shivachev B, Gilliland D, Pianella F, Ceccone G, Cotogno G, Rauscher H, Gibson N, Stamm H. Synthetic amorphous Silicon dioxide NM-200, NM-201, NM-202, NM-203, NM-204: Characterisation and physico-chemical properties. JRC repository: NM-series of representative manufactured nanomaterials. JRC Science and Policy Report. EUR 26046 EN, 2013.

90. Rasmussen K, Mast J, De Temmerman PJ, Verleysen E, Waegeneers N, van Steen F, Pizzolon JC, De Temmerman L, van Doren E, Alstrup Jensen K, Birkedal R, Levin M, Hjortkjær Nielsen S, Kalevi Koponen I, Clausen PA, Kofoed-Sørensen V, Kembouche Y, Thieriet N, Spalla O, Guiot C, Rousset D, Witschger O, Bau S, Bianchi B, Motzkus C, Shivachev B, Dimowa L, Nikolova R, Nihtianova D, Tarassov M, Petrov O, Bakardjieva S, Gilliland D, Pianella F, Ceccone G, Spampinato V, Cotogno G, Gibson N, Gaillard C, Mech A. Titanium dioxide NM-100, NM-101, NM-102, NM-103, NM-104, NM-105: Characterisation and physico-chemical properties. JRC repository: NM-series of representative manufactured nanomaterials. JRC Science and Policy Report, EUR 26637 EN, 2014.

91. Schippritt D, Lipinski HG, Wiemann M. Measurement of nanoparticle uptake by alveolar macrophages: A new approach based on quantitative image analysis. In: Wohlleben W, Kuhlbusch T, Schnekenburger J, Lehr C-M, editors. Nanomaterials Throughout their Lifecycles: Safety. Boca Raton: Human Hazard and Exposure. Taylor & Francis; 2014.

92. Desch CE, Dobrina A, Aggarwal BB, Harlan JM. Tumor necrosis factor-alpha exhibits greater proinflammatory activity than lymphotoxin in vitro. Blood. 1990;75:2030–4.

93. Cooper JA, Saracci R, Cole P. Describing the validity of carcinogen screening tests. Br J Cancer. 1979;39:87–9.

94. Rozman KK, Doull J. The role of time as a quantifiable variable of toxicity and the experimental conditions when Haber's c x t product can be observed: implications for therapeutics. J Pharmacol Exp Therap. 2001;296:663–8.

95. Tran CL, Buchanan D, Cullen RT, Searl A, Jones AD, Donaldson K. Inhalation of poorly soluble particles. II. Influence of particle surface area on inflammation and clearance. Inhal Toxicol. 2000;12:1113–26.

96. Duffin R, Tran L, Brown D, Stone V, Donaldson K. Proinflammogenic effects of low-toxicity and metal nanoparticles in vivo and in vitro: highlighting the role of particle surface area and surface reactivity. Inhal Toxicol. 2007;19:849–56.

97. Nel AE, Mädler L, Velegol D, Xia T, Hoek EMV, Somasundaran P, Klaessig F, Castranova V, Thompson M. Understanding biophysicochemical interactions at the nano-bio interface. Nat Mater. 2009;8:543–57.

98. Oberdörster G. Safety assessment for nanotechnology and nanomedicine: concepts of nanotoxicology. J Int Med. 2009;267:89–105.

99. Braakhuis HM, Park MV, Gosens I, De Jong WH, Cassee FR. Physicochemical characteristics of nanomaterials that affect pulmonary inflammation. Part Fibre Toxicol. 2014;11:18.

100. Senna M. Determination of effective surface area for the chemical reaction of fine particulate materials. Part & Part Systems Charact. 1989;6(163):167.

101. Stacy BD, King EJ, Harrison CV. Tissue changes in rats' lungs caused by hydroxides, oxides and phosphates of aluminium and iron. J Pathol Bacteriol. 1959;77:417–26.

102. Seiler F, Rehn B, Rehn S, Hermann M, Bruch J. Quartz exposure of the rat lung leads to a linear dose response in inflammation but not in oxidative DNA damage and mutagenicity. Am J Respir Cell Mol Biol. 2001;24:492–8.

103. Lindenschmidt RC, Driscoll KE, Perkins MA, Higgins JM, Maurer JK, Belfiore KA. The comparison of a fibrogenic and two nonfibrogenic dusts by bronchoalveolar lavage. Toxicol Appl Pharmacol. 1990;102:268–81.

104. Krewski D, Yokel RA, Nieboer E, Borchelt D, Cohen J, Harry J, Kacew S, Lindsay J, Mahfouz AM, Rondeau V. Human health risk assassment for aluminium, aluminium oxide, and aluminium hydroxide. J Toxicol Environ Health B Crit Rev. 2007;10(Suppl 1):1–269.

105. Warheit DB, Carakostas MC, Hartsky MA, Hansen JF. Development of a short-term inhalation bioassay to assess pulmonary toxicity of inhaled particles: comparison of pulmonary responses to carbonyl iron and silica. Toxicol Appl Pharmacol. 1991;107:350–68.

106. Henderson RF, Driscoll KE, Harkema JR, Lindenschmidt RC, Chang IY, Maples KR, Barr EB. A comparison of the inflammatory response of the lung to inhaled versus instilled particles in F344 rats. Fundam Appl Toxicol. 1995;24:183–97.

107. Roursgaard M, Poulsen SS, Poulsen LK, Hammer M, Jensen KA, Utsunomiya S, Ewing RC, Balic-Zunic T, Nielsen GD, Larsen ST. Time-response relationship of nano and micro particle induced lung inflammation. Quartz as reference compound. Hum Exp Toxicol. 2010;29:915–33.

108. Reuzel PG, Bruijntjes JP, Feron VJ, Woutersen RA. Subchronic inhalation toxicity of amorphous silicas and quartz dust in rats. Food Chem Toxicol. 1991;29:341–54.

109. Seiler F, Rehn B, Rehn S, Bruch J. Evidence of a no-effect level in silica induced rat lung mutagenicity but not in fibrogenicity. Arch Toxicol. 2001;74:716–9.

110. Bellmann B. 14-day nose-only inhalation toxicity study of Z-COTE HP1 in Wistar WU rats. 02 G 09 005 (draft report). Fraunhofer ITEM, Germany (study owner: Cefic, Belgium), 2011.

111. Keller J, Wohlleben W, Ma-Hock L, Strauss V, Gröters S, Küttler K, Wiench K, Herden C, Oberdörster G, van Ravenzwaay B, Landsiedel R. Time course of lung retention and toxicity of inhaled particles: short-term exposure to nano-Ceria. Arch Toxicol. 2014;88:2033–59.

112. Organisation for Economic Co-operation and Development (OECD). Series on the safety of manufactured nanomaterials. No. 51. Dossier on silicon dioxide (NM 200), ENV/JM/MONO(2015)14/PART1, 2015.

113. Organisation for Economic Co-operation and Development (OECD). Series on the safety of manufactured nanomaterials. No. 51. Dossier on silicon dioxide (NM 203), ENV/JM/MONO(2015)14/PART4, 2015.

114. Landsiedel R, Schnekenburger J, Alessandrini F, Buesen R, Haase A, Luch A, Ma-Hock L, Wiemann M. *nanoGEM final project report* (Gemeinsamer Abschlussbericht nanoGEM). Chapter 6. Work package 4 (AP4): Nanoparticle toxicology: Material properties and effects. 2014. doi:10.2314/GBV:82774322X **(project report in German)**.

115. Ankley GT, Bennett RS, Erickson RJ, Hoff DJ, Hornung MW, Johnson RD, Mount DR, Nichols JW, Russom CL, Schmieder PK, Serrrano JA, Tietge JE, Villeneuve DL. Adverse outcome pathways: a conceptual framework to support ecotoxicology research and risk assessment. Env Toxicol Chem. 2010;29:730–41.

116. Sager TM, Castranova V. Surface area of particle administered versus mass in determining the pulmonary toxicity of ultrafine and fine carbon black: comparison to ultrafine titanium dioxide. Part Fibre Toxicol. 2009;6:15.

117. Ho M, Wu KY, Chein HM, Chen LC, Cheng TJ. Pulmonary toxicity of inhaled nanoscale and fine zinc oxide particles: mass and surface area as an exposure metric. Inhal Toxicol. 2011;23:947–56.

Wiemann *et al. J Nanobiotechnol* (2016) 14:16

Page 27 of 27

118. Donaldson K, Schinwald A, Murphy F, Cho WS, Duffin R, Tran L, Poland C. The biologically effective dose in inhalation nanotoxicology. Acc Chem Res. 2013;46:723–32.

119. Braakhuis HM, Cassee FR, Fokkens PH, de la Fonteyne LJ, Oomen AG, Krystek P, de Jong WH, van Loveren H, Park MV. Identification of the appropriate dose metric for pulmonary inflammation of silver nanoparticles in an inhalation toxicity study. Nanotoxicol. 2015;23:1–11.

120. Simkó M, Nosske D, Kreyling WG. Metrics, dose, and dose concept: the need for a proper dose concept in the risk assessment of nanoparticles. Int J Environ Res Public Health. 2014;11:4026–48.

121. Organisation for Economic Co-operation and Development (OECD). Guidance document on acute inhalation toxicity testing. Series on testing and assessment. No. 39, ENV/JM/MONO(2009)28, 2009.

122. Donaldson K, Borm PJA, Oberdörster G, Pinkerton KE, Stone V, Tran CL. Concordance between in vitro and in vivo dosimetry in the proinflammatory effects of low-toxicity, low-solubility particles: the key role of the proximal alveolar region. Inhal Toxicol. 2008;20:53–62.

123. Ma J, Mercer RR, Barger M, Schwegler-Berry D, Cohen JM, Demokritou P, Castranova V. Effects of amorphous silica coating on cerium oxide nanoparticles induced pulmonary responses. Toxicol Appl Pharmacol. 2015;288:63–73.

124. Monteiller C, Tran L, MacNee W, Faux S, Jones A, Miller B, Donaldson K. The pro-inflammatory effects of low-toxicity low-solubility particles, nanoparticles and fine particles, on epithelial cells in vitro: the role of surface area. Occup Environ Med. 2007;64:609–15.

125. Johnston H, Brown DM, Kanase N, Euston M, Gaiser BK, Robb CT, Dyrynda E, Rossi AG, Brown ER, Stone V. Mechanism of neutrophil activation and toxicity elicited by engineered nanomaterials. Toxicol In Vitro. 2015;29:1172–84.

126. Chen J, Patil S, Seal S, McGinnis JF. Rare earth nanoparticles prevent retinal degeneration induced by intracellular peroxides. Nat Nanotechnol. 2006;1:142–50.

127. Arya A, Sethy NK, Singh SK, Das M, Bhargava K. Cerium oxide nanoparticles protect rodent lungs from hypobaric hypoxia-induced oxidative stress and inflammation. Int J Nanomed. 2013;8:4507–20.

128. Shehata N, Meehan K, Leber D. Study of fluorescence quenching in aluminum-doped ceria nanoparticles: potential molecular probe for dissolved oxygen. J Fluoresc. 2013;23:527–32.

129. Marzaioli V, Aguilar-Pimentel JA, Weichenmeier I, Luxenhofer G, Wiemann M, Landsiedel R, Wohlleben W, Eiden S, Mempel M, Behrendt H, Schmidt-Weber C, Gutermuth J, Alessandrini F. Surface modifications of silica nanoparticles are crucial for their inert versus proinflammatory and immunomodulatory properties. Int J Nanomed. 2014;9:2815–32.

130. Panas A, Marquardt C, Nalcaci O, Bockhorn H, Baumann W, Paur HR, Mülhopt S, Diabaté S, Weiss C. Screening of different metal oxide nanoparticles reveals selective toxicity and inflammatory potential of silica nanoparticles in lung epithelial cells and macrophages. Nanotoxicol. 2013;7:259–73.

131. Elliott GR, van Batenburg MJ, Bonta IL. Copper modulation of macrophage cyclooxygenase metabolite synthesis. Prostaglandins. 1987;34:657–67.

132. Kim JS, Peters TM, O'Shaughnessy PT, Adamcakova-Dodd A, Thorne PS. Validation of an in vitro exposure system for toxicity assessment of air-delivered nanomaterials. Toxicol In Vitro. 2013;27:164–73.

133. Ahamed M, Akhtar MJ, Alhadlaq HA, Alrokayan SA. Assessment of the lung toxicity of copper oxide nanoparticles: current status. Nanomed. 2015;10:2365–77.